



Metallogeny, structural evolution, post-mineral cover distribution and exploration in concealed areas of the northern Chilean Andes



M. García ^{a,b,*}, V. Maksaev ^b, B. Townley ^{b,a}, J. Dilles ^c

^a Advanced Mining Technology Center, Universidad de Chile, Av. Tupper 2007, Santiago, Chile

^b Departamento de Geología, Universidad de Chile, Plaza Ercilla 803, Santiago, Chile

^c College of Earth, Ocean and Atmospheric Sciences, Oregon State University, Corvallis, OR, USA

ARTICLE INFO

Article history:

Received 5 April 2016

Accepted 30 January 2017

Available online 30 March 2017

Keywords:

Geologic evolution

Mining exploration

Metallogenic belts

Porphyry-copper

Substratum depth

ABSTRACT

Mineral exploration of prospective areas concealed by extensive post-mineralization cover is growing, being very complex and expensive. The projection of rich and giant Paleocene to early Oligocene porphyry-Cu-Mo belts in northernmost Chilean Andes (17.5–19.5°S) has major exploration potential, but only a few minor deposits have been reported to date, due to the fact that the area is largely covered by post-mineral strata. We integrate the Cenozoic stratigraphic, structural and metallogenic evolution of this sector, in order to identify the most promising regions related to lesser post-mineral cover and the projection of different metallogenic belts. The Paleocene to early Eocene metallogenic belt extends along the Precordillera, with ca. 30 km wide, and includes porphyry-Cu prospects and small Cu (\pm Mo-Au-Ag) vein and breccia-pipe deposits. Geochronological data indicate an age of 55.5 Ma for an intrusion related to one deposit and ages from 69.5 to 54.5 Ma for hydrothermal alteration in one porphyry-Cu prospect and largest known Cu deposits. The middle Eocene to early Oligocene porphyry belt, in the Western Cordillera farther east, is associated with 46–44 Ma intrusions. It is estimated to be 40-km wide, but is largely concealed by thick post-mineral cover. The youngest Miocene to early Pliocene metallogenic belt, also in the Western Cordillera, is well-exposed and includes Au-Ag epithermal and polymetallic veins and manto-type deposits.

The Oligocene-Holocene cover consists of a succession of continental sedimentary and volcanic rocks that overall increase in thickness from 0 to 5000 m, from west to east. These strata are subhorizontal in the west and folded-faulted towards the east. Miocene gentle anticlines and monoclinal flexures extend along strike for 30–60 km in the Precordillera and were generated by propagation of high-angle east-dipping blind reverse faults with at least 300–900 m of Oligocene bedrock offset. The thickness of cover exceeds 2000 m in the eastern Central Depression, whereas it is generally less than 1000 m in the Precordillera along the Paleocene to early Eocene porphyry-Cu belt and it can reach locally up to 5000 m in the Western Cordillera, above the middle Eocene to early Oligocene belt.

In the studied Andean segment, the Miocene to early Pliocene metallogenic belt is superimposed on the Paleocene to Oligocene belts in a 40–50 km wide zone. This overlap may be explained by an accentuated migration of the magmatic front, from east to west, since ca. 25 Ma, as a consequence of subduction slab steepening after a period of magmatic lull and flat subduction from ca. 30–35 to 25 Ma. The identified areas of lesser cover thickness are prone to exploration for concealed deposits, especially along the projection of major porphyry-Cu-Mo belts.

© 2017 Elsevier B.V. All rights reserved.

1. Introduction

Traditional exploration of ore-deposits has been focused on deep or lateral extensions of exposed ore-bodies, where the geological mapping is a fundamental tool for targeting (Brimhall

et al., 2006). However, the depletion of these areas and recent discoveries and exploitation of deposits at depths greater than 1000 m (e.g., Superior district; Manske and Paul, 2002), as well as new drilling technologies, advances in deep-penetrating geophysics and geochemistry and better predictive geological models, are allowing access to deeper environments and large concealed areas (Sillitoe and Thompson, 2006). Mining and exploration of deposits becomes increasingly expensive with depth because of increased waste to ore ratios and underground block cave methods

* Corresponding author at: Advanced Mining Technology Center, Universidad de Chile, Av. Tupper 2007, Santiago, Chile.

E-mail address: mgarciaodoy@ing.uchile.cl (M. García).

are required. Nonetheless, locally high ore grades in certain metallic belts, as in central Andes, are enough to sustain underground mining. The exploration of deep concealed targets is very complex and there is little geologic documentation on how to explore for such targets efficiently, although it is clear that a multidisciplinary strategy and a good base of integrated geo-scientific knowledge are needed (Bennett et al., 2014; McCuaig and Hronsky, 2014). As there is a present reasonable economic depth of drilling, concealed targets can be quickly filtered or prioritized provided depth of cover is known, allowing better criteria for decisions on mine concession acquisitions, plan geophysical and geochemical surveys and/or definition of drilling programs. Zones with bedrock located at a depth of less than 500–1000 m may be suitable for exploration, whereas deeper zones can be ruled out in the current exploration economics.

In the Central Andes, three extensive Cenozoic longitudinal metallogenic belts contain the largest copper concentrations around the world (Figs. 1 and 2; Sillitoe, 1988, 1992; Zappettini et al., 2001; Camus, 2003; Sillitoe and Perelló, 2005; Maksaev et al., 2007). Each belt developed progressively and globally from west to east and represents discrete metallogenic periods. The westernmost Paleocene to early Eocene (62–51 Ma) belt is 30–50 km wide and includes mainly porphyry Cu-Mo deposits, and

minor copper mineralized tourmaline breccia pipes, enargite-bearing and Fe oxide-Cu-Au veins, epithermal precious metals deposits, and porphyry Cu-Au prospects. The largest porphyry Cu-Mo deposits of this belt are located in southern Peru, at Cerro Verde-Santa Rosa, Cuajone, Quellaveco and Toquepala, whereas in northern Chile, the main deposits are Mocha, Cerro Colorado, Spence and Lomas Bayas (Fig. 2). The middle Eocene to early Oligocene (43–31 Ma) belt varies in width from 130 km in southern Peru to 30–50 km in northern Chile, and includes mainly porphyry Cu deposits, with Mo and/or Au, and skarn deposits (Sillitoe, 1988; Perelló et al., 2003; Sillitoe and Perelló, 2005; Maksaev et al., 2007). The foremost deposits are in Chile (Collahuasi-Quebrada Blanca, Chuquicamata, Escondida and El Salvador; Fig. 2), and are associated with rich supergene enriched zones, and exotic Cu deposits (Münchmeyer, 1996; Sillitoe, 2005). The easternmost Miocene to early Pliocene (20–4 Ma) belt is wider, up to 400 km, extends along Peru, Bolivia, Chile and Argentina, and contains a variety of mineralization types, including Cu-Au-(Ag) and Cu-Mo porphyry deposits, skarn deposits, enargite carbonate replacements, high-sulfidation Au-Ag epithermal deposits and red-bed copper deposits (Sillitoe and Perelló, 2005).

We studied a segment of northern Chile, between 17.5 and 19.5°S latitudes, where the physiographic units are parallel to the

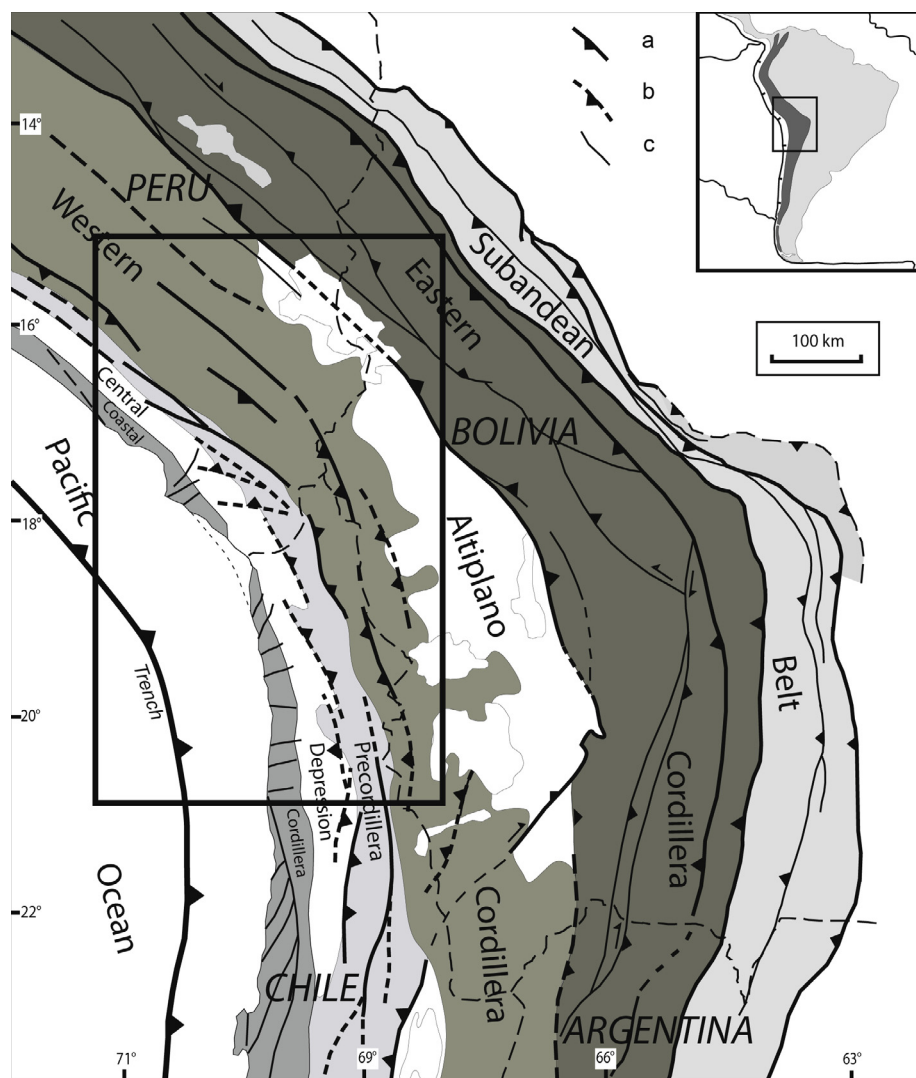


Fig. 1. Physiographic units of the central Andes, in Perú, Bolivia and Chile showing the location for Fig. 2 (inset box). (a) Neogene major fault, (b) Neogene inferred or blind fault, and (c) Neogene minor fault.

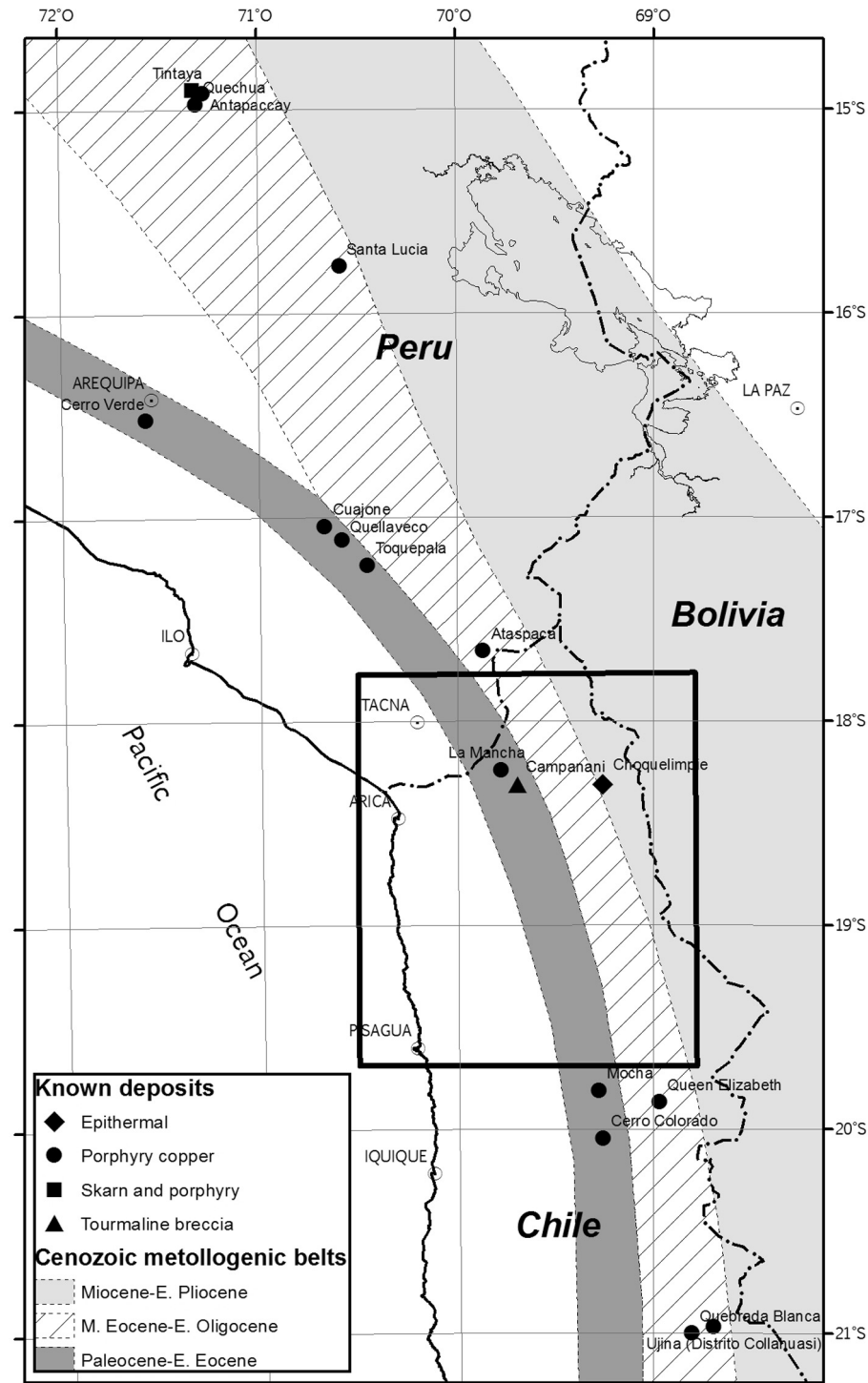


Fig. 2. Cenozoic metallogenic belts of the central Andes as defined by the ages of main deposits (based on Perelló et al., 2003 and Sillitoe and Perelló, 2005). Location of the study area (Fig. 3 inset) is also indicated.

Andean orogen and correspond to, from west to east: Coastal Cordillera, Central Depression, Precordillera and Western Cordillera (Figs. 1 and 3). The Coastal Cordillera is up to 25 km wide with elevation up to 1575 m and presents a uniform surface (Mortimer and Saric, 1972). The Central Depression is 40–55 km wide and its flat topography increases in altitude eastward from 500–1100 to 1900–2300 m, which gives a mean slope of 1–2°W. The Precordillera is 20–50 km wide, has a gently dipping surface, and reaches elevations up to 3200–3700 m. The Western Cordillera extends

east of Chile, to the Bolivian Altiplano (Figs. 1 and 3), and presents an irregular and elevated topography. In the Chilean part of the Western Cordillera, the altitude varies from 3200 to 6350 m, with summits corresponding to Miocene to Holocene stratovolcanoes. The western part of the area is dissected by deep exoreic valleys (Lluta, Azapa, Vitor, Camarones and Tiliviche-Camiña valleys; Fig. 3; Mortimer, 1980; García et al., 2011; Kirk-Lawlor et al., 2013). In the Coastal Cordillera and Central Depression, valley incisions are up to 1000 m, whereas in the Precordillera these are up to

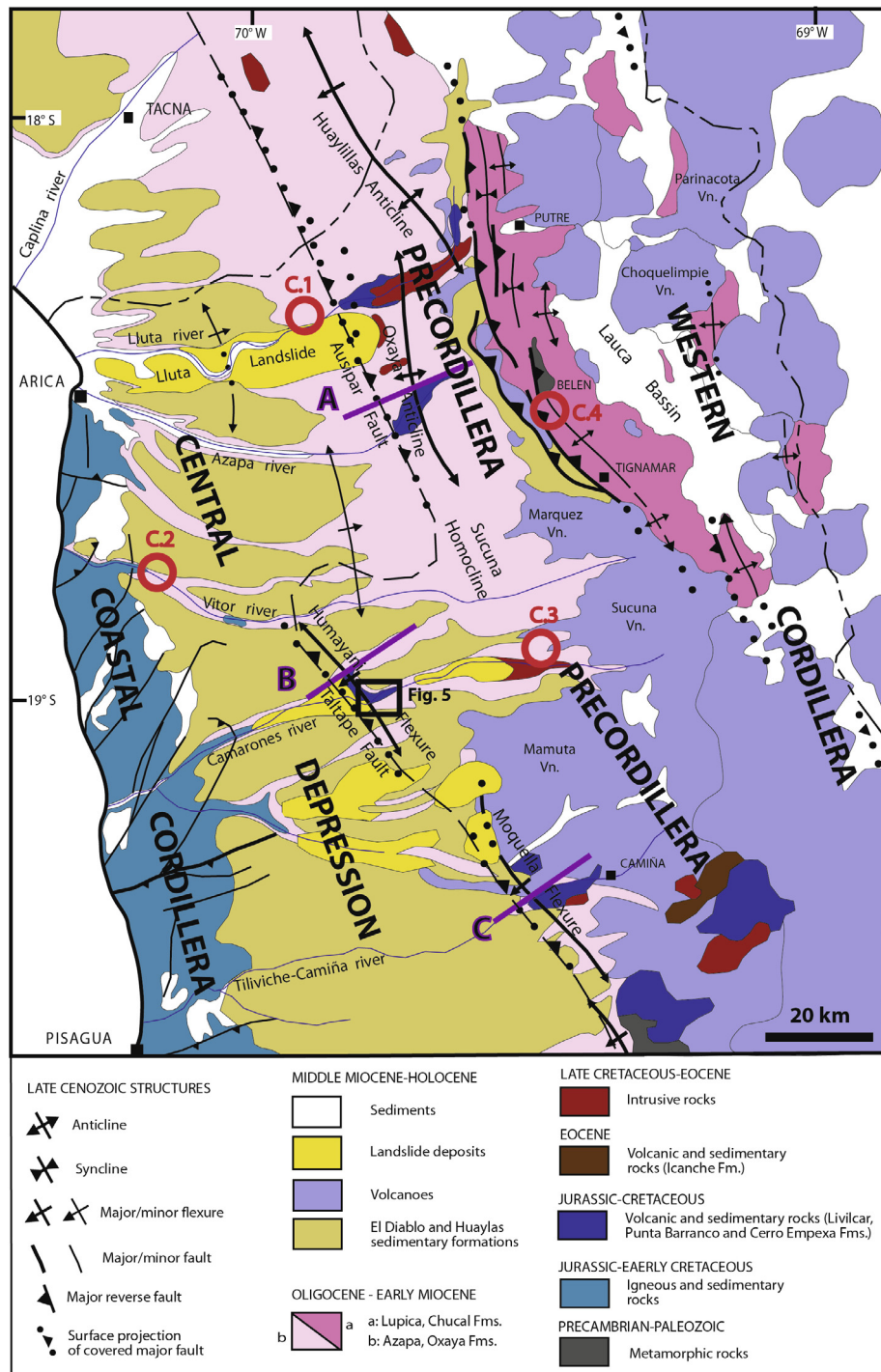


Fig. 3. Simplified geological map of northernmost Chile, showing distribution of main lithostratigraphic units, Late Cenozoic major structures, and location of stratigraphic columns (red circles, C1 to C4, in Fig. 5), detailed geological map (in Fig. 6) and studied cross sections (A, B and C, in Fig. 9).

1700 m. The studied area is located in the northern-central part of the hyper-arid Atacama Desert, where yearly mean precipitation ranges from 0.1 to 0.5 mm at the coast to 300 mm in the Western Cordillera (New et al., 2002; Strecker et al., 2007). The onset of extremely arid conditions in the western central Andes was in the middle Miocene (Rech et al., 2006; Arancibia et al., 2006; Evenstar et al., 2009; Jordan et al., 2014) and have favored the preservation of oxidized mineralization zones above and/or adjacent to the Paleogene porphyry copper deposits (Alpers and

Brimhall, 1988; Sillitoe and McKee, 1996; Bouzari and Clark, 2002; Quang et al., 2005).

The northernmost Chilean Andes (17.5–19.5°S) encompasses a portion of the giant Paleocene to early Oligocene porphyry-Cu-Mo belts (Fig. 2), however only small Cu-(Mo-Au-Ag) deposits and porphyry-Cu prospects are known. Either the region lacks porphyry-Cu mineral deposits or such deposits are concealed beneath an extended and thick Oligocene-Holocene post-mineral cover (Figs. 2 and 3). The geology of the region is well-mapped at

a scale 1:50,000 and supported by petrographic, geochemical, geochronological and metallogenic data (Wörner et al., 2000a; García et al., 2004, 2011, 2012, 2013; Pinto et al., 2004; Ordóñez and Rivera, 2004; García and Fuentes, 2012; Valenzuela et al., 2014; Cortés et al., 2014; Morandé et al., 2015). In this paper, we present and integrate geologic data including the Cenozoic stratigraphy, structural geology and mineral deposits. The goal is determine areas of shallow post-mineral cover rocks that might be amenable to exploration and provide an improved estimate of the distribution of the Andean metallogenic belts.

2. Stratigraphy

In the northernmost Chile, a regional angular unconformity separates a Late Proterozoic to Eocene bedrock from an Oligocene to Holocene rock cover, and provides a convenient stratigraphic marker (Figs. 3 and 4). Within the stratigraphic context, the youngest bedrock units include Late Cretaceous to Eocene intrusions that are related to major porphyry copper-molybdenum mineralization nearby in the Andes. Additionally, the composition and distribution of thickness of the Oligocene to Holocene post-mineral cover is crucial to defining potential areas amenable to future mining exploration.

2.1. Late proterozoic to eocene bedrock

Bedrock includes Late Proterozoic to Paleozoic metamorphic rocks, Jurassic to Cretaceous volcanic, sedimentary and intrusive rocks, and Late Cretaceous to Eocene volcanic and intrusive rocks (Figs. 3–7). The Late Proterozoic to Cambrian Belén Metamorphic Complex (Pacci et al., 1980a; Lucassen et al., 2000; Basei et al., 1996; Wörner et al., 2000b; Loewy et al., 2004; García et al., 2004) and the Late Devonian to Early Carboniferous Quebrada Aroma Metaturbiditic Complex (García, 1967; Harambour, 1990; Morandé et al., 2015) are exposed in the westernmost part of the High Cordillera and Precordillera, respectively (Figs. 3 and 4). Jurassic to Early Cretaceous marine fossiliferous sedimentary strata are also present in the Precordillera (Livilcar Formation, Muñoz et al., 1988; García et al., 2004; and Longacho Formation, Galli and Dingman, 1962; Morandé et al., 2015). Middle to Late Jurassic marine volcanic and sedimentary rocks and Late Jurassic and Early Cretaceous intrusive rocks are largely exposed in the Coastal Cordillera (Figs. 3 and 4; Cecioni and García, 1960; Salas et al., 1966; Muzzio, 1986; García et al., 2004). Early Cretaceous continental red conglomerates and sandstones in the Coastal Cordillera unconformably overlie the Jurassic units and are conformably overlain by middle Cretaceous andesitic lavas and continental sandstones and by middle Cretaceous marine sedimentary rocks (Muzzio, 1986; García and Fuentes, 2012). Early Cretaceous continental sedimentary and andesitic rocks crop out locally in the western Precordillera (Punta Barranco Formation; Figs. 4 and 6; García et al., 2013; Valenzuela et al., 2014) and early Late Cretaceous (100–85 Ma) quartz monzodiorites and granodiorites form a restricted and discontinuous NW-trending belt (Figs. 6 and 7; García et al., 2004, 2013). Late Cretaceous (74–66 Ma) continental volcanic rocks are present in the Precordillera (Cerro Empexa Formation; Fig. 4; Galli and Dingman, 1962; García et al., 2013; Valenzuela et al., 2014).

Late Cretaceous to Paleocene intrusions crop out in the Precordillera and cut the Jurassic-Cretaceous formations (Figs. 3, 4, 5 and 7). In the northern Precordillera, large bodies of coarse-to-fine-grained amphibole-biotite-bearing granodiorites, quartz monzodiorites, quartz monzonites and quartz diorites have yielded several U-Pb and K-Ar ages between 66 ± 2 and 54.5 ± 1.3 Ma (Table 1; Muñoz and Charrier, 1996; García et al., 2004) and geochemical

analyses indicate a high-K calc-alkaline affinity (García et al., 2004). In the southern Precordillera, discrete bodies of medium-to-fine-grained intrusions include pyroxene-amphibole-biotite diorites with a U-Pb zircon age of 69.5 ± 1.3 to 66.6 ± 0.8 Ma and biotite-amphibole granites with U-Pb zircon ages of 66.3 ± 0.5 to 61.7 ± 0.7 Ma (Fig. 7; Table 1; García et al., 2013; Valenzuela et al., 2014). To the north, in southernmost Peru, early-middle Paleocene porphyry copper-related intrusions have been dated between 62 and 60 Ma in the Lluta-Palca District (Fig. 7; Wilson and García, 1962; Clark et al., 1990; Acosta et al., 2011) and between 65.1 and 53.5 Ma in the Cuajone-Toquepala Cluster (Sillitoe and Mortensen, 2010; Simmons et al., 2013). The composition and ages of Paleocene porphyry copper-related intrusions are similar in southern Peru and northernmost Chile.

Eocene rocks locally crop out in the Western Cordillera, in the northernmost and southernmost sectors of the study area (Figs. 3, 4 and 7). In the southernmost sector, the early Eocene continental andesitic volcanic rocks (Icanche Formation; Maksaev, 1978) have been dated by U-Pb zircon at 49.6 ± 0.53 Ma (Valenzuela et al., 2014). There, the Cretaceous and Eocene formations are intruded by medium-grained amphibole-biotite (\pm pyroxene) granodiorites, which have yielded a U-Pb zircon age of 44.4 ± 0.5 Ma and a K-Ar biotite age of 46.3 ± 1.3 Ma (Figs. 3, 4 and 7; Table 1; Argandoña, 1984; Harambour, 1990; Valenzuela et al., 2014). In the northernmost sector of the study area, the Eocene rocks are intrusions of mainly medium-grained amphibole-biotite-bearing granodiorites and quartz monzodiorites that are in part foliated. These have Rb-Sr, K-Ar and Ar-Ar ages of 46.1 ± 2.8 , 35 ± 3 , 36.0 ± 0.9 and 31.8 ± 1.0 Ma, but 46.1 Ma is considered as the crystallization age, whereas 36–32 Ma are considered as minimum ages associated with deformation and/or hydrothermal alteration (Table 1; Pacci et al., 1981; García et al., 2012). Thus, the Eocene intrusions in the study area have ages restricted to 46.3–44.4 Ma and minimum ages of 36–32 Ma. The geochemical composition of the Eocene intrusions is compatible with high-K calc-alkaline affinity (García et al., 2012; Valenzuela et al., 2014). To the north of the study area, in southernmost Peru, middle Eocene intermediate composition intrusions, with ages of 46.6–39.2 Ma, are related to currently-mined porphyry-copper deposits (Fig. 2; Wilson and García, 1962; Clark et al., 1990; Acosta et al., 2011).

2.2. Oligocene to holocene cover rocks

The Oligocene to Holocene cover rocks are extensive, occupying surface outcrops over most of the study area (Figs. 3, 4 and 5). The rocks and unconsolidated deposits are predominantly continental sedimentary and volcanic in origin and include andesitic-dacitic stratovolcanoes, variably preserved from the early Miocene, and local hypabyssal intrusions. The cover thickness is highly variable, ranging from 0 to 250 m in the Coastal Cordillera to maxima of more than ca. 5000 m in the Western Cordillera. In the Central Depression and Precordillera, the fluvial, alluvial and pyroclastic rocks dip horizontally and gently west or are gently folded (Azapa, Oxaya, El Diablo and Huaylas formations), whereas in the Western Cordillera, the effusive, pyroclastic, alluvial and locally lacustrine rocks are moderately to strongly folded and faulted (Lupica, Utayane, Chucal, Chojña, Macusa, Joracane, Condoriri, Puchuldiza and Lauca formations, and the Lauca Ignimbrite; Figs. 3, 4, 5 and 6; Salas et al., 1966; Tobar et al., 1968; Mortimer et al., 1974; Lahsen, 1982; Naranjo and Paskoff, 1985; Kött et al., 1995; Muñoz and Charrier, 1996; Wörner et al., 2000a; García et al., 2004, 2011, 2012, 2013; Pinto et al., 2004; Cortés et al., 2014; Valenzuela et al., 2014).

The Azapa Formation consists of up to 500 m of fluvial conglomerates and sandstones (Figs. 3, 4, 5 and 6). The lower sandstones have yielded detrital U-Pb zircon ages greater than 35 Ma whereas

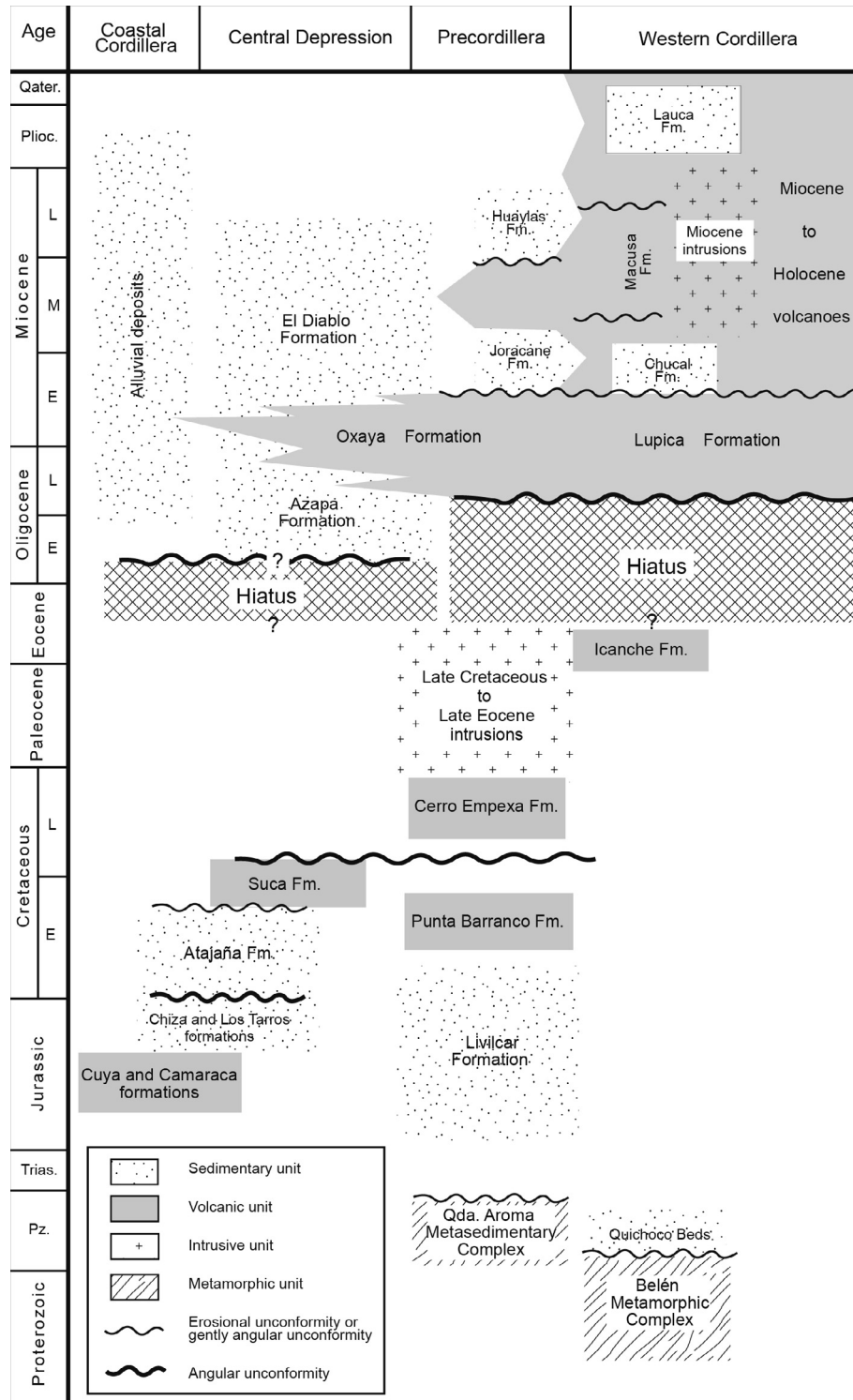


Fig. 4. General stratigraphic chart of the study area, showing distribution, composition, age and contact relationships of units.

the upper sandstones have ages greater than 30 Ma (Wotzlaw et al., 2011). This unit is conformably overlain by the tuffs of the Oxaya Formation, which have ages between 25 and 17 Ma (see compilation in García et al., 2004), therefore, the age of the Azapa Formation is restricted to the Oligocene and probably the late Eocene. The Oxaya Formation is composed of extensive ignimbritic rhyolitic tuffs and sedimentary rocks, which are up to 1000 m thick in the Precordillera and up to 20 m thick in the western Central

Depression (Figs. 3–6). This unit is overlain conformably by up to 400 m thick lacustrine, fluvial and alluvial sandstones, siltstones, limestones and gravels of the El Diablo Formation (16–9 Ma). In the eastern Precordillera, the Oxaya Formation is overlain by Miocene andesitic stratovolcanoes or relics of these (e.g., 20–17 Ma Cordón Quevilque, 15–13 Ma Mamuta, 15–12 Ma Sucuna and 11–9 Ma Marquez volcanoes) and by the middle-late Miocene fluvial deposits of the Huaylas Formation (Figs. 3–6).

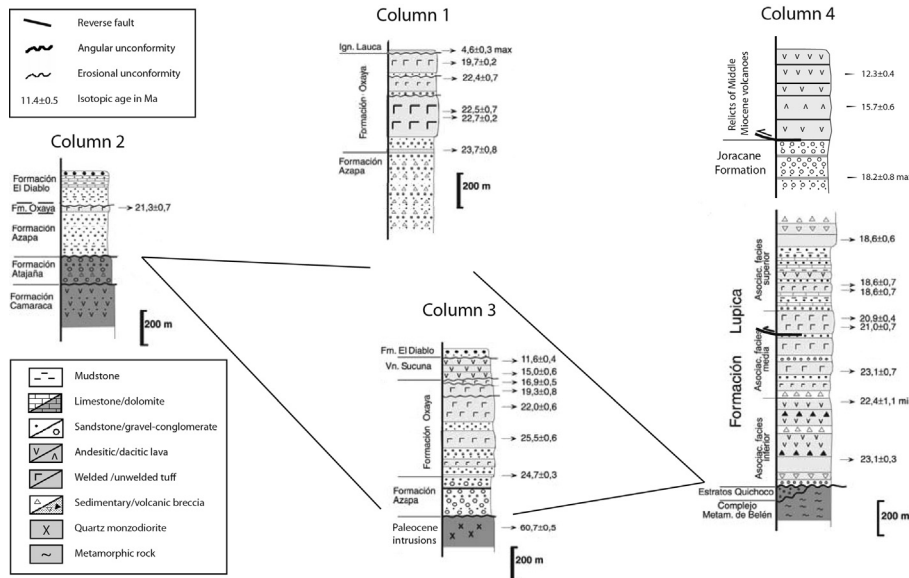


Fig. 5. Stratigraphic columns of the Oligocene to Holocene cover rocks, showing name, thickness, composition and age control of units and their spatial variations. The isotopic ages are mainly K-Ar (from García et al., 2004; see text). Location of columns in Fig. 3.

North to south variations of Oligocene to Holocene stratigraphy are also pronounced. In the northern part of the Western Cordillera east of Arica, the Lupica Formation consists of an up to 2500 m thick sequence of andesitic and dacitic lavas, rhyolitic tuffs and alluvial and lacustrine sedimentary rocks (Figs. 3–5). Previous studies of this unit have presumed a Late Cretaceous to Tertiary age by correlation (Salas et al., 1966); however, geochronology indicates ages ranging between 25 and 18 Ma (García, 1996, 2002; García et al., 2000, 2004, 2012). The formation is overlain in angular unconformity, in part progressively, by restricted alluvial, fluvial and lacustrine sedimentary rocks (Chucal, Macusa, Joracane and Lauca formations, and ca. 2.8 Ma Lauca Ignimbrite) and by middle Miocene to Holocene andesitic-dacitic stratovolcanoes (Fig. 5). To the south, east of Pisagua, the Late Oligocene to Early Miocene volcanic and sedimentary rocks (Utayane, Chojña and Condoriri formations) are covered progressively by middle Miocene to Pliocene sedimentary rocks and ignimbrites and by late Miocene to Holocene andesitic-dacitic stratovolcanoes (Lahsen, 1982; Cortés et al., 2014; Valenzuela et al., 2014). Each stratovolcano can contribute up to 2000 m of thickness to the Oligocene-Holocene cover. The Lupica, Utajape and Chojña formations are intruded by middle-late Miocene diorite to monzonite and dacitic, hypabyssal, porphyritic and holocrystalline stocks (Figs. 4 and 7; Wörner et al., 1988; García et al., 2004; Cortés et al., 2014). East of Arica, these rocks have U-Pb and K-Ar ages of 16.0 ± 0.6 , 12.5 ± 0.6 and 6.6 ± 0.2 Ma (Table 1) and are in part related to Ag, Pb, Zn and Sb mineralization and hydrothermal alteration (see below).

3. Metallogeny

The Cenozoic metallic ore deposits of northernmost Chile ($17.5\text{--}19.5^\circ\text{S}$) form part of three important Andean metallogenic belts: the Paleocene to early Eocene (62–50 Ma) and middle Eocene to early Oligocene (43–31 Ma) porphyry Cu-Mo belts and the Miocene to Early Pliocene polymetallic belt (20–4 Ma) (Fig. 2; Sillitoe, 1988, 1992; Zappettini et al., 2001; Camus, 2003; Sillitoe and Perelló, 2005; Maksaev et al., 2007). In the study area, the Paleocene to early Eocene belt occurs along the Precordillera whereas the middle Eocene to early Oligocene and Miocene to early Plio-

cene belts along the Western Cordillera (Fig. 8; Salas et al., 1966; Pacci et al., 1980b; García et al., 2004, 2012, 2013; Ordóñez and Rivera, 2004; Valenzuela et al., 2014). Additionally, two small copper veins (Tal tape and Sta. Ana) and one porphyry-Cu prospect have been recognized in the westernmost Precordillera, are hosted in the Early Cretaceous rocks and are spatially close to mid Cretaceous intrusions (Figs. 6–8; Table 2; Salas et al., 1966; Saric and Mortimer, 1971; Pacci et al., 1980b; García et al., 2013). These Cretaceous deposits are not considered further in the metallogeny. None of the deposits in the area are exploited to date.

3.1. 1- Paleocene to early eocene belt

The Paleocene to early Eocene metallogenic belt is ca. 30 km wide and represented by veins, breccia-pipes and vein-stockworks, containing copper, copper-molybdenum, copper-gold-silver and silver-lead-zinc mineralization (Fig. 8; Table 2; Salas et al., 1966; Pacci et al., 1980b; García et al., 2004, 2013; Ordóñez and Rivera, 2004). Two prospects of porphyry-Cu type and several Cu occurrences are also known (Table 2). The deposits are mainly hosted by the Late Cretaceous to Paleocene intrusions and Cretaceous stratigraphic sequences (Punta Barranco and Cerro Empexa formations). The largest vein-type deposit is Dos Hermanos that contains inferred resources of 500,000 tonnes at 1 wt % Cu and 120 ppm Mo, whereas other veins (as Rosario, Jamiralla and Eva II) have smaller volumes but higher grades of Cu (10–18 wt%) and Au (10–19 ppm) (Fig. 8; Table 2; Salas et al., 1966; Pacci et al., 1980b). The Campanani deposit is a tourmaline-bearing breccia-pipe and vein-stockwork that contains inferred resources of up to 100,000 tonnes of mainly oxidized copper ores at 1 wt% Cu with anomalous Au and Ag values (Salas et al., 1966; Pacci et al., 1980b; Ordóñez and Rivera, 2004). The host-rock is a quartz monzodiorite with a U-Pb zircon age of 55.5 ± 1.0 Ma and a K-Ar age on hydrothermal biotite of 54.5 ± 1.3 Ma (Fig. 7; Table 1; García et al., 2004). In the Jamiralla vein deposit, a K-Ar sericite age of 56.1 ± 1.4 Ma indicates a Late Paleocene age for mineralization (Fig. 7; Tables 1 and 2; Ordóñez and Rivera, 2004). Southward, some copper occurrences or prospects (Sin Nombre, Quistagama and Camiña) are spatially close to dioritic and granitic intrusions with ages ranging from 67 to 62 Ma (Figs. 7 and 8; Tables 1 and

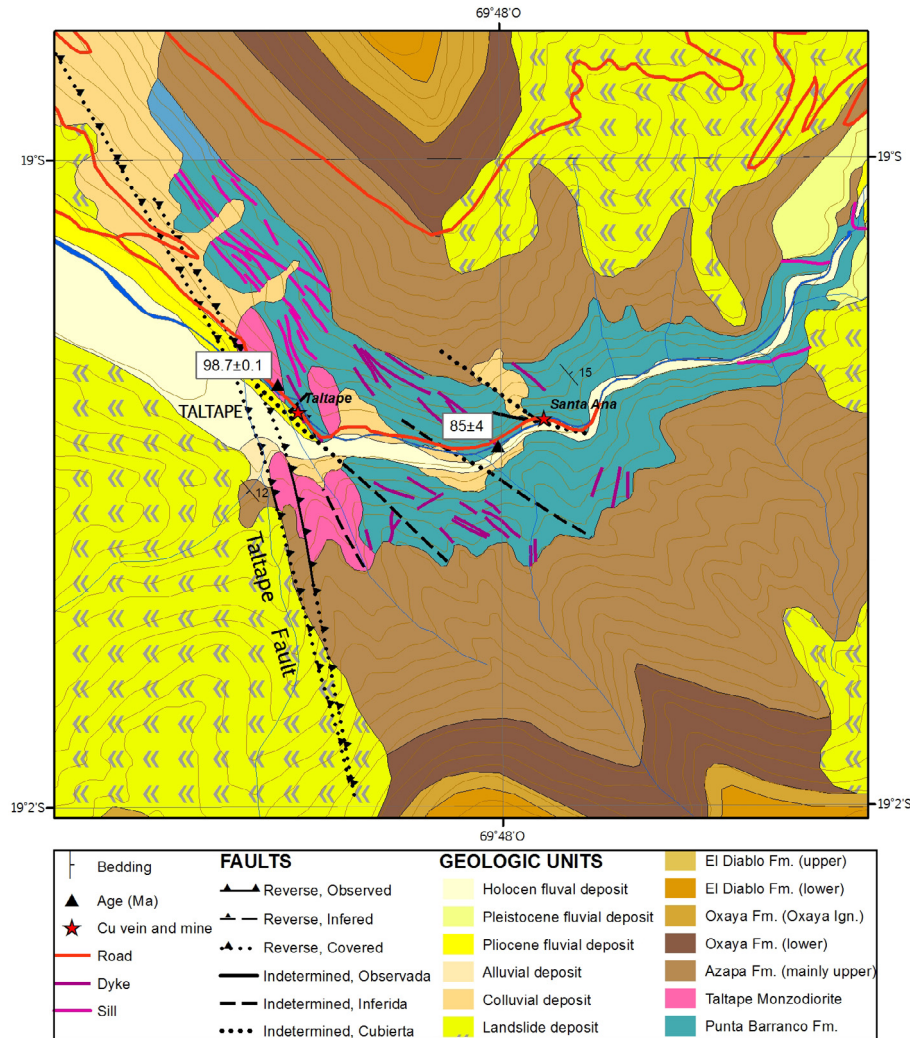


Fig. 6. Detailed geological map of the Taltape area, in the Camarones valley, showing the style of the used available field data; scale 1:25.000 and coordinates in WGS-1984. See area location in Fig. 3. The Early Cretaceous volcanic rocks (Punta Barranco Formation) are intruded by the 99 Ma Taltape Monzodiorite and dykes and sills. In the western part of the map, the Taltape reverse fault outcrops and is responsible that the Cretaceous rocks be exposed in the central-eastern part. Note also the differentiation of rock units in the Oligocene-Miocene cover. Based on García et al. (2004) at north of 20°S and García et al. (2013) at south of 20°S.

2; García et al., 2013; Valenzuela et al., 2014). The southernmost vein deposits (El Chino, Sapte, La Hedionda San Pedro and Quebrada Guacesiña) include Ag-(Pb-Zn) ores without isotopic ages and are preliminarily assigned to the Paleocene belt (Fig. 8; Tables 2; Pacci et al., 1980b; Ordóñez and Rivera, 2004).

Two porphyry-Cu prospects (La Mancha and Camarones) occur in this belt (Fig. 8; Table 2). The La Mancha (or Palmani) prospect, north of the Lluta valley, is buried beneath 700 m of post-mineral cover. Small surface outcrops of hydrothermally-altered andesitic rocks intruded by granodiorite contain zones of high density quartz ± limonite ± oxide copper and quartz-sericite-pyrite veinlets, corresponding to early A-type and late D-type veinlets, respectively (H. Munster, written commun., 2014; following the classification of Gustafson and Hunt, 1975). An age of 51 Ma has been preliminarily mentioned for the La Mancha prospect (Sillitoe and Perelló, 2005). The Camarones (or Chilpe) porphyry-Cu prospect (Fig. 8) underlies a 600 m thick post-mineral cover and was initially recognized by Pacci (1978) and Pacci et al. (1980b) as a zone of hydrothermal alteration and hornfels hosted in Cretaceous volcanic rocks, intruded by a granodiorite porphyry dikes. Within the prospect area a 300 m long and 0.8–2 m thick copper-bearing vein has been previously mined (Ordóñez and Rivera, 2004). The

host-rock of this vein contains disseminated mineralization of chalcopyrite and supergene chalcocite (up to 3 and 1 vol.%, respectively) and well as oxide malachite and chalcanthite. The andesite host rock contains pervasive potassio alteration to secondary mineral assemblages of biotite ± quartz ± magnetite ± pyrite, whereas felsic hosts rocks contain local zones of phylllic-argillic alteration with quartz ± sericite ± kaolinite assemblages. An inferred resource of 10 million tonnes at 0.2 wt% copper has been estimated (Fig. 8; Table 2; Pacci et al., 1980b). Sericite-bearing altered rocks have K-Ar whole rock ages of 67 ± 3 and 72 ± 3 Ma, which suggest an average age of ca. 69.5 Ma (Fig. 7; Table 1; García et al., 2004; Ordóñez and Rivera, 2004).

3.2. Middle eocene to early oligocene belt

This middle Eocene to early Oligocene metallogenic belt is poorly defined in the Western Cordillera because most bedrock is concealed by abundant and thick post-mineral cover. Only one ore deposit is known (Guacesiña), in the southernmost part of the study area (Fig. 8; Table 2; Pacci et al., 1980b; Ordóñez and Rivera, 2004). This is a small Ag-(Pb, Zn, Cu) vein hosted in a probable Eocene intrusion lacking isotopic date. In the Eocene intru-

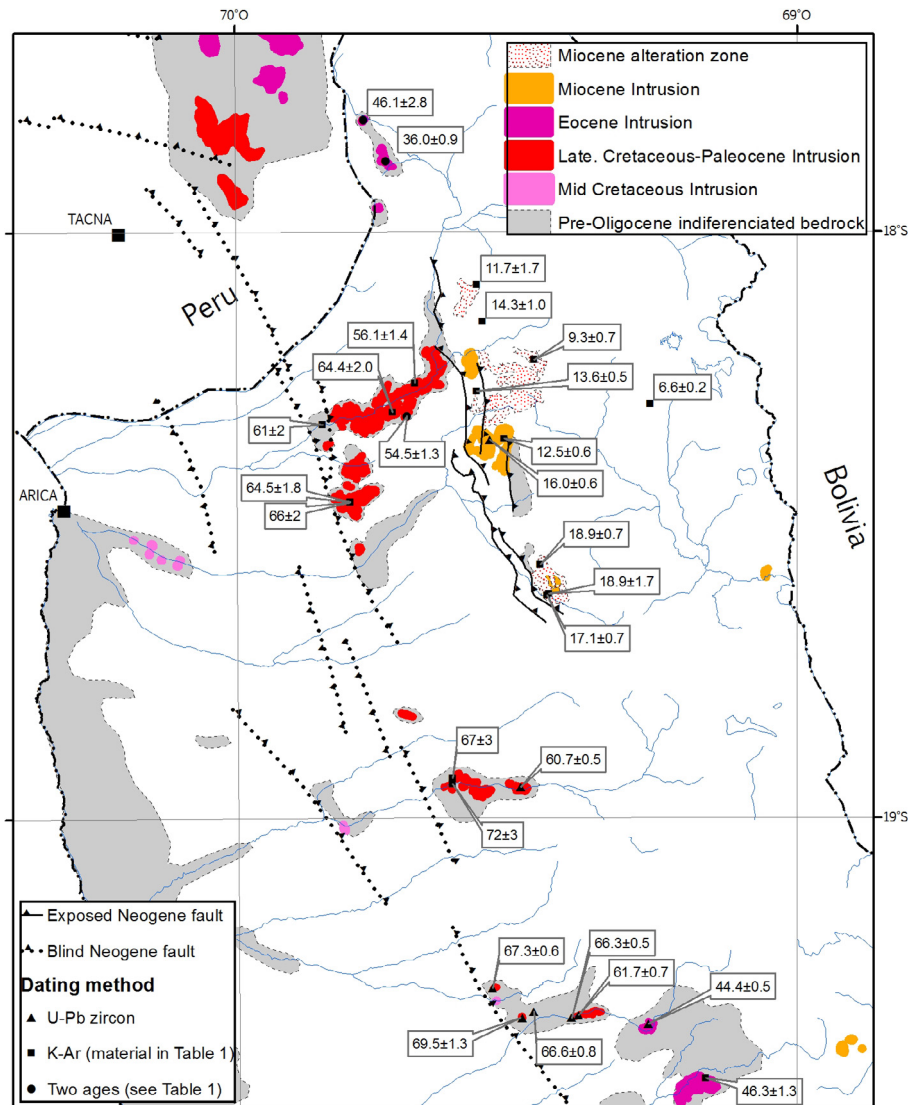


Fig. 7. Simplified map showing distribution and ages of middle Cretaceous to Miocene intrusive rocks, outcrops of pre-Oligocene rock units, and Neogene major faults. For more detail of ages, see Table 1. Outcrops of the pre-Oligocene bedrock and intrusive rocks were gently exaggerated for better visualization purposes. Outcrops of southern Peru were taken from Acosta et al. (2011).

sions of the northernmost part of the area, K-Ar and Ar-Ar ages of 36 to 32 Ma are considered as minimum ages associated with deformation and/or hydrothermal alteration (Table 1; Pacci et al., 1981; García et al., 2012), which is compatible with latest Eocene mineralization in the rest of the Andes. To the north and south of the study area, the middle Eocene to early Oligocene porphyry-Cu belt is well developed (Fig. 2; Zappettini et al., 2001; Camus, 2003; Perelló et al., 2003; Sillitoe and Perelló, 2005). Immediately north and south of the study area, the belt includes the 46–39 Ma Ataspaca and Tarata districts in southernmost Peru (Clark et al., 1990; Acosta et al., 2011) and the 38–37 Ma Queen Elizabeth porphyry-Cu prospect in northern Chile (Camus, 2003; Sillitoe and Perelló, 2005), respectively. Therefore, due to discontinuous and limited exposure in the study area this belt of potential porphyry Cu mineralization can only be estimated to be approximately 40 km wide after projections from north and south.

3.3. 3- Miocene to early pliocene belt

The Miocene to early Pliocene metallogenic belt in the study region includes the epithermal Choquelimpie Au-Ag deposit, the

Ag, Pb, Zn, Cu and Sb Belén-Tignámar district and several polymetallic prospects (Fig. 8; Table 2). Choquelimpie is the most voluminous deposit, and contains high-sulfidation epithermal mineralization mainly as veins and hydrothermal breccias characterized by electrum, argentite, argentiferous galena, realgar and sphalerite (Sánchez, 1970; Bisso, 1991; Gröpper et al., 1991). The deposit was formed in a 7–8 Ma andesitic-dacitic volcano and mineralization can be temporally related to dacitic dykes dated at 6.6 ± 0.2 Ma (Fig. 8; Table 2; Aguirre, 1990; Wörner et al., 1988). The resource has been estimated in 56 Mt at 1.1 g/t Au and 16.9 g/t Ag (Cecioni et al., 2000).

The Belén-Tignámar district is formed by several small polymetallic deposits that include predominantly Ag, Pb and Zn (\pm Cu-Mo) veins, Cu (\pm Ag) veins and mantos, and subordinately Sb(\pm Sn) veins (Fig. 8; Table 2; Salas et al., 1966; Sayes, 1977; Pacci et al., 1980b; Ordóñez and Rivera, 2004). The individual resources of polymetallic deposits are less than 300,000 tonnes ore (as Santa Rosa, Guanaco, Churicala Sur) that contains locally high grades of up to 1100 g/t Ag, 16 wt% Pb, 20 wt% Zn, 19 wt% Sb and 6 wt% Cu (Table 2). The Tignámar prospect is a Cu-Mo quartz vein-stockwork, with inferred 200,000 tonnes ore containing 2 wt% Cu, and has been

Table 1

Summary of isotopic ages of the Late Cretaceous to Miocene intrusive and hydrothermally-altered rocks of northernmost Chilean Andes, between 17.5 and 19.5°S. See plot in Fig. 7.

Sample	Geological unit	Approximative location	Coordinate UTM E'	Coordinate UTM N'	Lithology	Method and material	Edad ± error (Ma ± 2σ)	Comment/Interpretation	Reference
<i>Late Cretaceous to Paleocene intrusions and hydrothermal alteration zones</i>									
110520	Camarones alteration zone	Chilpe	4,35,139	79,05,458	–	K-Ar whole rock U-Pb zircon	72 ± 3 69.5 ± 1.3	Alteration age (sericitization)	Ordóñez and Rivera (2004)
CAM25	Ks diorites	Qda. Camiña	4,48,256	78,61,291	Microdiorite	U-Pb zircon	67.3 ± 0.6		Valenzuela et al. (2014)
FR-2	Suca Diorite	Qda. de Suca	4,42,745	78,66,940	Diorite	U-Pb zircon	67.3 ± 0.6		García et al. (2013)
MAL-102	Camarones alteration zone	S Pachica	4,35,145	79,06,540	Sericitized tuff (?)	K-Ar whole rock U-Pb zircon	67 ± 3 66.6 ± 0.8	Alteration age (sericitization)	García et al. (2004)
BL-13	Ks diorites	Qda. Camiña	4,50,485	78,62,460	Diorite dyke	U-Pb zircon	66.6 ± 0.8		Valenzuela et al. (2014)
C-7	Qda. Retamilla Granite	Qda. Retamilla	4,57,577	78,61,445	Quartz Monzodiorite	U-Pb zircon	66.3 ± 0.5		Valenzuela et al. (2014)
MAL-157	Lluta intrusions	Qda. Cardones	4,15,865	79,58,575	Quartz Monzodiorite	K-Ar biotite	66 ± 2		García et al. (2004)
NMG-434-1	Lluta intrusions	Qda. Cardones	4,15,795	79,58,639	Diorite	K-Ar biotite	64.5 ± 1.8		Muñoz (written commun.)
NMG-434-2	Lluta intrusions	Qda. Lluta	4,23,815	79,75,625	Diorite	K-Ar biotite	64.4 ± 2.0	K low, unreliable age	Muñoz and Charrier (1996)
C-3	Qda. Retamilla Granite	Qda. Retamilla	4,58,911	78,61,876	Granite	U-Pb zircon	61.7 ± 0.7		Valenzuela et al. (2014)
MAL-152	Lluta intrusions	W Aranche	4,10,595	79,73,239	Basalt dyke	K-Ar whole rock U-Pb zircon	61 ± 2 60.7 ± 0.5	Probably minimum age	García et al. (2004)
MAL-2	Esquiña intrusions	Esquiña	4,47,965	79,04,926	Quartz Monzonite	U-Pb zircon	60.7 ± 0.5		García et al. (2004)
110508	Jamiralla alteration zone	Mina Jamiralla	4,28,063	79,81,167	–	K-Ar sericite	56.1 ± 1.4	Alteration age (sericitization)	Ordóñez and Rivera (2004)
MAL-117	Lluta intrusions	Mina Campanane	4,26,515	79,74,875	Quartz Monzodiorite	U-Pb zircon	55.5 ± 1.0		García et al. (2004)
MAL-117	Lluta intrusions	Mina Campanane	4,26,515	79,74,875	Quartz Monzodiorite	K-Ar biotite	54.5 ± 1.3		García et al. (2004)
<i>Eocene intrusions</i>									
HA.01	Qda. Aroma Granodiorite	Qda. Retamilla	4,82,805	78,49,983	Monzogranite	K-Ar biotite	46.3 ± 1.3		Harambour (1990)
ARI-2	Eocene intrusions	Pampa Jaillave, N C° Tawaicoñuñu	4,18,450	80,31,150	Granodiorite	Rb-Sr isochron whole rock	46.1 ± 2.8		Pacci et al. (1981)
BL-01	Qda. Aroma Granodiorite	Qda. Aroma	4,72,085	78,60,256	Granodiorite	U-Pb zircon	44.4 ± 0.5		Valenzuela et al. (2014)
MAL-246	Eocene intrusions	W Humapalca	4,22,731	80,23,405	Granodiorite	K-Ar biotite	36.0 ± 0.9	Excess of 40Ar. Probably deformation or alteration age	García et al. (2012)
ARI-2	Eocene intrusions	Pampa Jaillave, N C° Tawaicoñuñu	4,18,450	80,31,150	Granodiorite	K-Ar biotite	35 ± 3	Probably deformation or alteration age	Pacci et al. (1981)
MAL-246	Eocene intrusions	W Humapalca	4,22,731	80,23,405	Granodiorite	Ar-Ar isochron biotite	31.8 ± 1.0	Initial 40Ar/36Ar of 550 ± 70. Minimum age	García et al. (2012)
<i>Miocene intrusions and hydrothermal alteration zones</i>									
110518	Lupica Fm. (hydrot. altered) in Churicala Norte Mine	Churicala Norte Mine	4,53,294	79,41,383	–	K-Ar whole rock	18.9 ± 1.7	Alteration age (sericitization)	Ordóñez and Rivera (2004)
110510	Lupica Fm. (hydrot. altered) in Santa Rosa Mine	Santa Rosa Mine	4,51,619	79,46,963	–	K-Ar whole rock	18.9 ± 0.7	Alteration age (sericitization)	Ordóñez and Rivera (2004)
MAL-214	Lupica Fm. (hydrot. altered) near Churicala Norte Mine	E Tignámar	4,52,965	79,41,069	Dacite	K-Ar whole rock	17.1 ± 0.7	Alteration age (sericitization)	García et al. (2004)
GAL-51	Miocene intrusions	Murmuntani	4,42,115	79,70,475	Quartz Monzodiorite-	U-Pb zircon	16.0 ± 0.6		García et al. (2004)

(continued on next page)

Table 1 (continued)

Sample	Geological unit	Approximative location	Coordinate UTM E	Coordinate UTM N*	Lithology	Method and material	Edad ± error (Ma ± 2σ)	Comment/ Interpretation	Reference
MAL-222	Lupica Fm. (hydrot. altered)	N Putre	4,40,745	79,92,808	Monzonite Andesite	K-Ar whole rock	14.3 ± 1.0	Chloritized rock. Alteration age	García et al. (2004)
753-G	Lupica Fm. (hydrot. altered)	E Socoroma	4,39,695	79,79,639	Tuff	K-Ar whole rock	13.6 ± 0.5	Alteration age (sericitization)	Gardeweg (1996)
NMG-443-2	Miocene intrusions	E Murmuntani	4,44,815	79,70,625	Dacite porphyry	K-Ar biotite	12.5 ± 0.6		Muñoz and Charrier (1996)
CAL-156	Lupica Fm. (hydrot. altered)	W C° Tapaca	4,39,720	79,99,700	Tuff (?)	K-Ar whole rock	11.7 ± 1.7	Alteration age (alunitization)	García et al. (2004)
762-G	Lupica Fm. (hydrot. altered)	N C° Vilanuñumani	4,50,415	79,85,608	Dacite	K-Ar whole rock	9.3 ± 0.7	Alteration age (alunitization)	Gardeweg (1996)
CHO 098	Miocene intrusions	Vn. Choquelimpie	4,72,343	79,77,293	Dacite dyke	K-Ar whole rock	6.6 ± 0.2		Wörner et al. (1988)

* Datum WGS-1984.

considered as a porphyry-type prospect (Pacci, 1970, 1977; Pacci et al., 1980b). The deposits and prospects of the Belén-Tignámar district are mainly hosted in the lower part of the Lupica Formation and are related to intrusion of middle Miocene (16–12 Ma) diorite to quartz-monzonite hypabyssal stocks (García et al., 2004). Sericitized rocks in the district have K-Ar whole rock ages between 17.1 ± 0.7 and 18.9 ± 1.7 Ma (Fig. 6; Table 1; García et al., 2004; Ordóñez and Rivera, 2004). Two copper vein-deposits (El Tranque and El Tranque Sur) hosted in the Belén Metamorphic Complex may be older but are here considered to be Miocene due to their proximity to other Miocene ore-deposits (Table 2).

To the north of Belén-Tignámar district and west of Putre, a large ($<250 \text{ km}^2$) zone of argillic and sericitic hydrothermal alteration affect rocks of the Lupica Formation and contains copper-molybdenum prospects (Pacci et al., 1980b). The altered rocks have K-Ar whole rock ages between 9.3 ± 0.7 and 14.3 ± 1.0 Ma (Fig. 7; Table 1; Gardeweg, 1996; García et al., 2004). To the NW of Putre, small Pliocene-Holocene manganese mantos are interpreted as genetically associated to sedimentary exhalative processes (Salas et al., 1966; Cruzat, 1967, 1970; Pacci et al., 1980b; García et al., 2004). In the southernmost Peru, immediately to the north of the study area, the Miocene to early Pliocene metallogenetic belt includes middle Miocene Au(-Ag) epithermal mineralization at both the Pucamarca deposit and Huilacollo prospect (Fig. 8; Acosta et al., 2011). Therefore, this belt is very wide and defined extensively along the northern Chile, southern Peru and western Bolivia.

4. Structural evolution

The rocks of the northernmost Chilean Andes ($17.5\text{--}19.5^\circ\text{S}$) have been deformed in various periods since the mid Cretaceous as evidenced by angular unconformities in strata and fault-cutting relationships. The main structures affecting the Oligocene to Holocene units strike N-S to NW-SE and some of these bound the physiographic units and control the slope variations (Figs. 3 and 9). Here, we emphasize evidence that allows for separation of distinct deformational periods, especially linked to the Eocene to Miocene structures that control (a) the exposure and preservation of blocks containing porphyry copper deposits and (b) the distribution and thickness of the post-mineral cover.

Early Eocene Icanche Formation rocks are folded and unconformably overlain by the late Oligocene-early Miocene Oxaya Formation (Valenzuela et al., 2014). Late Cretaceous to Paleocene intrusions in the Lluta valley are cut by NNE-trending subvertical strike-slip faults, and are also unconformably overlain by the Oxaya Formation (García et al., 2004). These relationships suggest that middle-late Eocene to probably as young as early Oligocene contractional and transcurrent deformation is likely part of the Domeyko Fault System in northern Chile and is linked to the Incalic contractional phase in Chile (Maksaev, 1979; Reutter et al., 1991, 1996; Maksaev and Zentilli, 1999; Tomlinson et al., 2001, 2015; Charrier et al., 2007, 2013; Mpodozis and Cornejo, 2012) and Peru (Noble et al., 1979; Mégard, 1984, 1987; Sébrier et al., 1988; Noblet et al., 1996).

Oligocene tectonic activity is observed in the western Precordillera, in blind steeply east-dipping reverse faults that are locally exposed in canyons below the latest Oligocene to Miocene rocks (Ausipar and Taltape faults; Figs. 3, 6 and 9; Muñoz and Charrier, 1996; García, 2002; García et al., 2004, 2013; García and Héral, 2005; Charrier et al., 2013). These faults were also active in the Miocene (see below), therefore, the Oligocene activity must be detected when the Miocene deformation is restored. The Taltape Fault is exposed in the Camarones valley, where strikes N20–30°W and dips 50–60°E, and secondary faults in the hanging wall show slickensides indicating reverse movement (García, 2002;

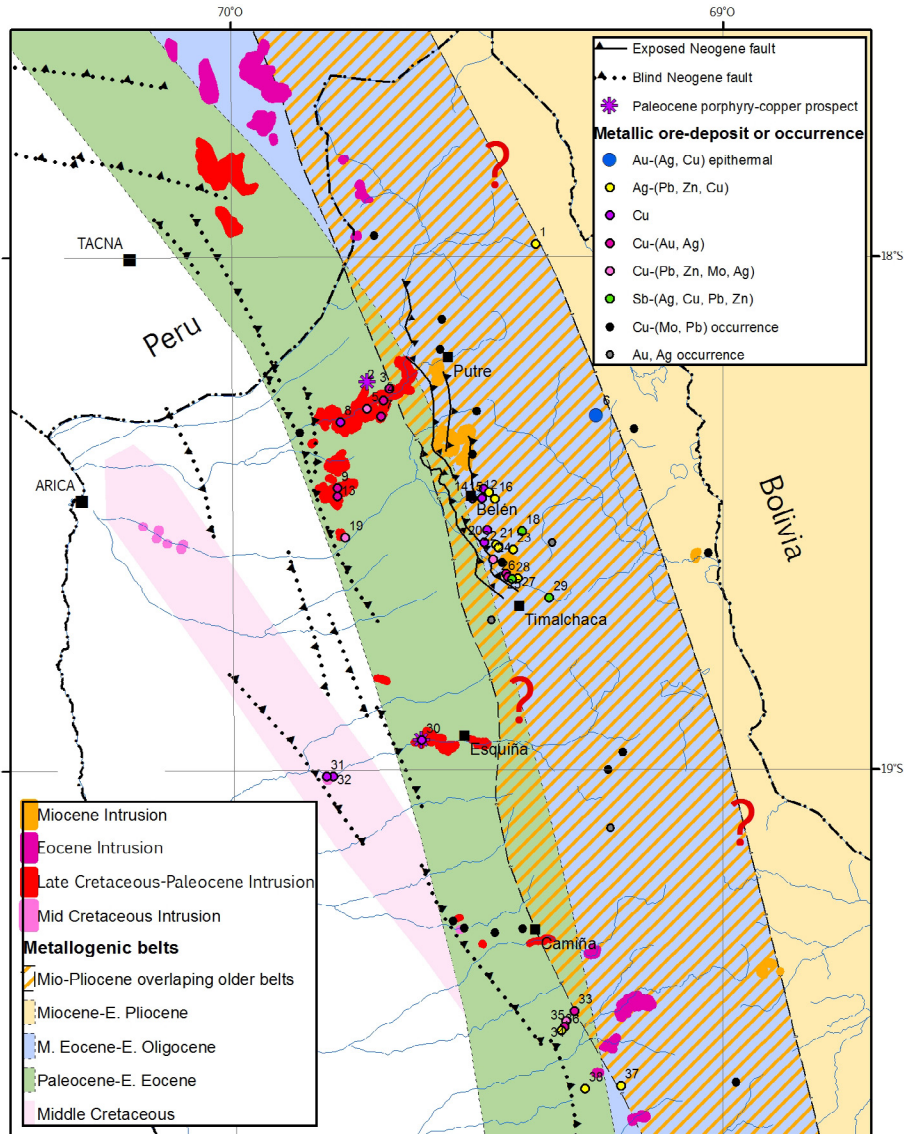


Fig. 8. Distribution of the middle Cretaceous to Pliocene metallic ore deposits and the intrusive and metallogenic belts. This includes vein-type, manto-type and vein-stockwork deposits, occurrences and porphyry-Cu prospects. Outcrops of the intrusive rocks were gently exaggerated for better visualization purposes. Outcrops of southern Peru were taken from [Acosta et al. \(2011\)](#).

[García et al., 2004, 2013](#)). The fault has reverse displacement of at least 300 m of Cretaceous rocks (Punta Barranco Formation and intrusions) atop the lower part of the Oligocene Azapa Formation. The upper part of the Azapa Formation is present on both sides of the fault and is not cut by the pre-Miocene fault, which indicates a reverse movement mainly during the Early Oligocene. The Ausipar Fault is exposed in the Lluta and Azapa valleys, where strikes N10–30°W and dips 50–70°E ([García, 2002; García et al., 2004; García and Héral, 2005](#)). Its hanging wall consists of the Jurassic-Early Cretaceous rocks that are locally unconformably overlain by the uppermost part of the Azapa Formation, whereas the footwall consists of a full thickness of Azapa Formation. The Oxaya Formation is on both sides of the fault, so the thin exposures of the Azapa Formation in the hanging wall indicate the existence of an Oligocene reverse faulting of at least 900 m.

Miocene to Holocene deformation is very minor in the Coastal Cordillera and Central Depression and is represented by a series of subvertical faults with a variety of strikes and displacements generally smaller than 200 m (except one displacement of

500 m) and by gentle and widely spaced folds and flexures with amplitudes less than 200 m ([Fig. 3; García et al., 2004; Allmendinger and González, 2010; García and Fuentes, 2012](#)). In the Precordillera, the present-day surface is gently folded in vast asymmetric west-vergent anticlines and flexures (monocline folds; [Figs. 3 and 9](#)). East of Arica, the Huayllillas and Oxaya anticlines have lengths of 60 and 50 km, and amplitudes of 950 and 850 m, respectively, and are bounded to the west by the relatively straight trace of the surface projection of the blind Ausipar Fault ([Figs. 3 and 9; Muñoz and Charrier, 1996; García et al., 2004; García and Héral, 2005](#)). The Oxaya Anticline has limbs dipping up to 25°W and 6°E, and growth strata on its eastern limb indicate that folding occurred between ca. 11.7 and 10.7 Ma. Across the fold, shortening (<100 m) is much less than its amplitude (<850 m), which suggests a steep dip of the Ausipar Fault at depth ([García and Héral, 2005](#)). To the south, the Precordillera is characterized by a surface that dips 2–3° west (Sucuna Monocline) that can be followed with minor structural interruption to the Central Depression where the surface dips 1–2° west ([Fig. 3](#)). To the south of 19 °S, the

Table 2

Summary of metallic ore deposits and Paleocene porphyry copper prospects related to the Mid Cretaceous to Miocene intrusions of the northernmost Chile. Note that minor occurrences and other prospects are not been considered in this table but they are plotted in Fig. 8.

No. in Fig. 8	Name	Coordinate UTM E'	Coordinate UTM N'	Metal	Type	Inferred resources (t)	Mean grade	Host rock, unit	References	Comments
<i>Mid Cretaceous belt</i>										
31	Taltape	4,14,651	78,97,535	Cu	Vein	5000	4% Cu	Punta Barranco Fm.	Salas (1966a), Salas et al. (1966), Saric and Mortimer (1971), Pacci et al. (1980b), Ordóñez and Rivera (2004)	Possible resources: 20,000 t with 2% Cu
32	Santa Ana	4,16,051	78,97,500	Cu	Vein	8000	4% Cu	Punta Barranco Fm.	Salas (1966b), Saric and Mortimer (1971), Pacci et al. (1980b), Ordóñez and Rivera (2004)	Possible resources: 1000 t with 5% Cu
<i>Paleocene-Early Eocene belt</i>										
2	La Mancha prospect	4,23,424	79,82,608	Cu	Stockwork			Cerro Empexa Fm. and Lluta intrusions (K-T)	H. Munster (written commun.)	
3	Jamiralla	4,28,063	79,81,167	Cu-(Au, Ag)	Vein, breccia pipe	4057	10 g/t Au; 15–18% Cu	Lluta intrusions (K-T)	Salas et al. (1966), Pacci et al. (1980b), Ordóñez and Rivera (2004)	
4	Rosario	4,26,795	79,78,639	Cu-(Au)	Vein, breccia pipe	500	15 g/t Au; 15–18% Cu	Lluta intrusions (K-T)	Salas et al. (1966), Pacci et al. (1980b), Ordóñez and Rivera (2004)	
5	Dos Hermanos	4,23,335	79,76,879	Cu-(Mo)	Stockwork	5,00,000	120 g/t Mo; 1% Cu	Lluta intrusions (K-T)	Salas et al. (1966), Pacci et al. (1980b), Ordóñez and Rivera (2004)	
7	Campanani	4,26,386	79,75,252	Cu-(Au, U)	Stockwork, vein, breccia pipe	1,00,000		Lluta intrusions (K-T)	Salas et al. (1966), Pacci et al. (1980b), García et al. (2004), Ordóñez and Rivera (2004)	
8	Eva II (o Chironta)	4,17,513	79,74,002	Cu	Vein	1000	10% Cu	Lluta intrusions (K-T)	Pacci et al. (1980b), Ordóñez and Rivera (2004)	
9	Lucita	4,16,958	79,59,811	Cu-(Ag, Au)	Vein	60,000	5% Cu	Lluta intrusions (K-T)	Pacci et al. (1980b), Ordóñez and Rivera (2004)	
13	Halcones	4,16,905	79,57,936	Cu-(Au, Ag)	Vein	50,000	6% Cu	Lluta intrusions (K-T)	Pacci et al. (1980b), Ordóñez and Rivera (2004)	
19	Santuario	4,18,595	79,49,139	Cu-(Pb, Zn, Mo, Ag)	Vein			Livilcar Fm.	Pacci et al. (1980b)	
30	Chilpe / Camarones prospect	4,35,139	79,05,458	Cu	Vein / stockwork	1,00,00,000	0.2–1% Cu	Suca or Punta Barranco Fm.	Pacci (1978), Pacci et al. (1980b), Ordóñez and Rivera (2004)	Resources are given for the Camarones porphyry-Cu prospect
33	El Chino	4,67,995	78,46,941	Cu-(Au)	Vein	2400		Cerro Empexa Fm.	Pacci et al. (1980b)	Possible resources: 4800 t
34	Sapte	4,66,281	78,44,816	Cu-(Pb, Zn, Ag)	Vein	60,000	125–150 g/t Ag; 3% Pb	Cerro Empexa Fm.	Pacci et al. (1980b), Ordóñez and Rivera (2004)	Possible resources: 240,000 t
35	La Hedionda	4,65,786	78,43,533	Cu-(Au)	Vein	3000	150 g/t Ag; 12.5% Pb	Cerro Empexa Fm.	Ordóñez and Rivera (2004)	
36	San Pedro	4,65,179	78,42,735	Ag-(Pb, Zn, Cu)	Vein			Cerro Empexa Fm.	Pacci et al. (1980b), Ordóñez and Rivera (2004)	Possible resources: 48,600 t
38	Quebrada Guacesiña	4,70,252	78,30,236	Ag-(Pb, Zn)	Vein	450		Qda. Aroma Metam. Complex and Cerro Empexa Fm.	Pacci et al. (1980b)	
<i>Middle Eocene-Early Oligocene belt</i>										
37	Guacesiña	4,78,002	78,30,846	Ag-(Pb, Zn, Cu)	Vein	1500	205 g/t Ag; 2.5% Au	Eocene(?) granodiorite-granite	Pacci et al. (1980b), Ordóñez and Rivera (2004)	Possible resources: 3000 t
<i>Miocene-Pliocene belt</i>										
1	Locura (o Colpita)	4,59,598	80,12,458	Ag-(Pb, Zn)	Manto	1500	700 g/t Ag; 0.5% Pb	Lupica Fm.	Pacci et al. (1980b), Ordóñez and Rivera (2004)	
6	Choquelimpie	4,72,674	79,75,539	Au-(Ag, Cu)	Vein, stockwork	5,60,00,000	1.1 g/t Au; 16.9 g/t Ag	Late Miocene volcano	Sánchez (1970), Bisso (1991), Gröpper et al. (1991), Cecioni et al. (2000), Ordóñez and Rivera (2004)	
10	El Tranque	4,48,399	79,59,656	Cu	Vein	500	6% Cu	Belén Metam. Complex	Sayes (1977), Pacci et al. (1980b), Ordóñez and Rivera (2004)	in siliceous dyke
11	San Lorenzo	4,49,524	79,58,890	Ag-(Cu,	Vein	40,000	357 g/t Ag; 16%	Lupica Fm.	Salas et al. (1966), Sayes (1977), Pacci et al.	Possible resources:

Table 2 (continued)

No. in Fig. 8	Name	Coordinate UTM E*	Coordinate UTM N*	Metal	Type	Inferred resources (t)	Mean grade	Host rock, unit	References	Comments
12	El Tranque Sur	4,48,339	79,58,856	Pb, Zn) Cu	Vein		Pb; 20% Zn	Belén Metam. Complex	(1980b), Ordóñez and Rivera (2004) This work	100,000 t with 300 g/t Ag in quartz(-sulfur) vein system
14	El Milagro	4,45,975	79,57,580	Cu	Manto	500	5% Cu	Lupica Fm.	Pacci et al. (1980b)	
15	Guanaco	4,48,058	79,57,542	Cu	Manto	2,25,000	3–6% Cu	Lupica Fm.	Sayes (1977), Pacci et al. (1980b), Calvo (1992), Ordóñez and Rivera (2004)	Possible resources: 20,000 t with 1% Cu
16	Patíño	4,50,827	79,57,531	Ag-(Pb, Zn, Cu)	Vein	10,000	200 g/t Ag	Lupica Fm.	Sayes (1977), Pacci et al. (1980b), Ordóñez and Rivera (2004)	
17	Sabinaya	4,49,243	79,50,797	Cu	Manto	240	4% Cu	Lupica Fm.	Pacci et al. (1980b), Ordóñez and Rivera (2004)	
18	Apacheta	4,56,695	79,50,539	Sb-(Ag, Mo)	Vein	10,000	19% Sb; 209 g/t Mo	Lupica Fm.	Sayes (1977), Pacci et al. (1980b), Ordóñez and Rivera (2004)	
20	Pumane	4,48,553	79,48,060	Cu	Vein	1000	1% Cu	Lupica Fm.	Pacci et al. (1980b), Ordóñez and Rivera (2004)	
21	Torpedo	4,51,125	79,47,595	Ag-(Cu, Pb, Zn)	Vein	6000	2.5% Cu	Lupica Fm.	Salas et al. (1966), Sayes (1977), Pacci et al. (1980b), Ordóñez and Rivera (2004)	
22	Santa Rosa	4,51,619	79,46,963	Ag-(Pb, Zn)	Vein	3,00,000	160 g/t Ag; 4 g/t Au	Lupica Fm.	Sayes (1977), Pacci et al. (1980b), Ordóñez and Rivera (2004)	
23	Chulpa	4,54,785	79,46,505	Ag-(Pb, Zn, Au)	Vein	5000	65 g/t Ag; 72% Pb; 5% Zn	Lupica Fm.	Sayes (1977), Pacci et al. (1980b), Ordóñez and Rivera (2004)	
24	Putagua	4,50,465	79,44,443	Cu-(Pb)	Vein	20,000	3% Cu	Lupica Fm.	Sayes (1977), Pacci et al. (1980b), Ordóñez and Rivera (2004)	
25	Churicala Norte	4,53,294	79,41,383	Cu-(Ag)	Vein	5000	200 g/t Ag	Lupica Fm.	Pacci et al. (1980b), Ordóñez and Rivera (2004)	
26	Churicala Sur	4,53,595	79,40,639	Cu-(Ag)	Vein	2,00,000	0.2% Cu; 88 g/t Ag	Lupica Fm.	Sayes (1977), Pacci et al. (1980b)	
27	Chivatune	4,55,770	79,40,378	Ag-(Pb, Zn, Cu)	Vein	50,000	250–350 g/t Ag; 16% Pb; 16% Zn	Lupica Fm.	Pacci et al. (1980b), Ordóñez and Rivera (2004)	Possible resources: 500,000 t
28	Capitana	4,54,471	79,40,191	Sb-(Ag, Cu, Pb, Zn)	Vein	5000	5–7% Sb; 2.5% Pb; 1080 g/t Ag; 5% Cu	Lupica Fm.	Salas et al. (1966), Sayes (1977), Pacci et al. (1980b), Ordóñez and Rivera (2004)	
29	Ociel	4,62,565	79,36,199	Sb-(Ag, Pb)	Vein	10,000	4.2 g/t Ag; 5% Sb	Lupica Fm.	Salas et al. (1966), Sayes (1977), Pacci et al. (1980b), Ordóñez and Rivera (2004)	

* Datum WGS-1984.

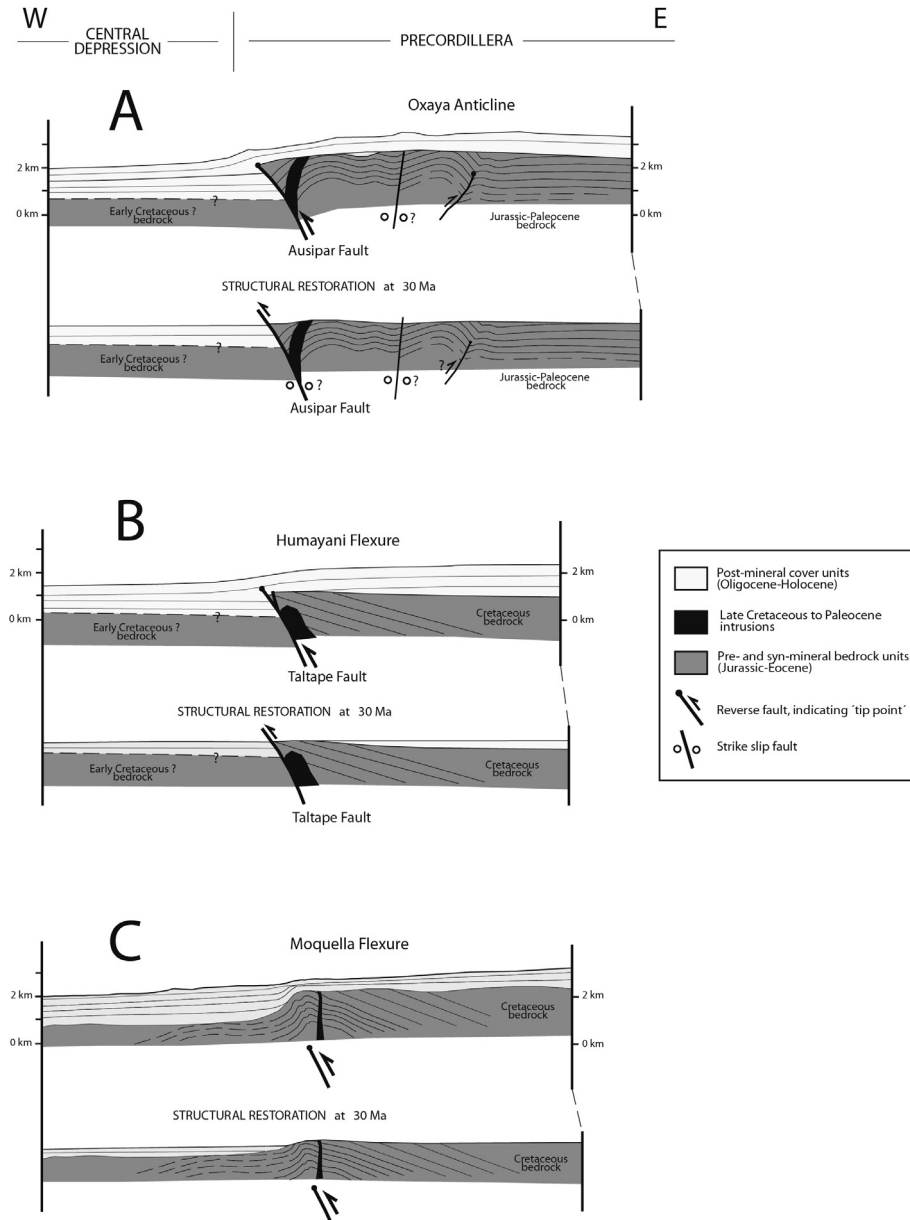


Fig. 9. Cross-sections in the western border of the Precordillera illustrating the Oxaya Anticline (A) and the Humayani (B) and Moquella (C) monocline flexures. Trace locations of cross-sections are in Figs. 3 and 10. Each section has its structural restoration at ca. 30 Ma, showing geological configuration after the formation of the Paleogene ore deposits.

Precordillera is bounded to the west by the Humayani, Moquella and Aroma-Soga flexures (Figs. 3 and 9), which produce a topographic step of up to 800 m. The 30 km long Humayani Flexure is related to activation and propagation of the blind Taltape Fault and was generated after deposition of the Middle Miocene El Diablo Formation (Figs. 3, 6 and 9; García, 2002). In the Moquella (40 km in long) and Aroma-Soga flexures, the amount of shortening is small and growth strata indicate a continuous contractional deformation during the late Oligocene-Miocene (~25 to ~6 Ma), but the controlling master faults have not been observed at surface (Pinto et al., 2004; Farías et al., 2005; García et al., 2013; Valenzuela et al., 2014). Kinematic forward models show that the deformation in the Moquella Flexure area can be produced by a single blind 65° east-dipping reverse fault that has a tip-line located at 3–4 km depth and has had several periods of movement since the middle Cretaceous (Riquelme, 2015). In summary, the

Miocene anticlines and flexures of the Precordillera show little shortening but important vertical displacements, and are interpreted as generated by propagation of east-dipping blind reverse faults, several of which are likely reactivated older basement faults (Fig. 9). Oligocene reverse faulting is also evidenced. In contrast, in the Western Cordillera, the Miocene to Holocene structures are partially exposed and form a fold-thrust belt with somewhat different character and vergency along the strike (Fig. 3). At the center, between Putre and Tignamar, the belt is west-vergent, involves the pre-Oligocene basement and has produced a W-E structural shortening of at least 10 km (Muñoz and Charrier, 1996; García, 2002; García et al., 2004; Charrier et al., 2013), whereas to the north and south, the belt is east-vergent, thin-skinned, and affects only the post-Oligocene cover sequence (Lahsen, 1982; Riquelme, 1998; García, 2002; García et al., 2004, 2012; Charrier et al., 2013; Cortés et al., 2014; Valenzuela et al., 2014).

5. Thickness variation of the post-mineral cover

Determination of lower thicknesses of the post-mineral cover is crucial to explore in covered areas. We have estimated the thickness variations for the Oligocene to Holocene cover that conceals much of the two Paleocene to early Oligocene porphyry-Cu-Mo metallogenic belts. Integration of all available geological and geo-physical information allowed construction of a cover thickness distribution map (Fig. 10). Although the metallogenic belts are along the Precordillera and Western Cordillera, the reviewing and compilation data for the Central Depression was also necessary.

In the Central Depression, the cover thickness increases progressively from west to east, being much smaller than 200 m in the Coastal Cordillera. In the southwestern part of the Central Depression, the cover thickness is of 432 m measured from one drill-hole (Fig. 10; Mordojovich, 1965). In the easternmost Central Depression, the cover-bedrock contact is not observed but a minimum cover thickness can be estimated: in the Lluta and Azapa val-

leys, the cover is at least 940 and 1020 m in thickness, respectively (Figs. 5 and 10); in the Camarones valley, the cover is at least 1040 m in thickness; in the Suca valley, the cover is at least 750 m in thickness. Additionally, the cover thickness in the Central Depression can be estimated from two reflection seismic profiles (Fig. 10). The transformation of vertical wave time arrival to depth in the reflection seismic profiles was contrasted respect to drill-hole information and the observations of the cover-bedrock contact in canyons in the western Central Depression. In the northern profile, the maximum thickness of cover is 1800 m approximately in the central part of the Central Depression, and in the eastern border of the profile, this diminishes to 400 m. In the southern profile, the maximum thickness of cover is 1700 m, and this is relatively constant in the entire central-eastern segment (Fig. 10). Considering the maximum thickness identified in the seismic profiles and the structural evolution of the Precordillera, we expect that the maximum depth of bedrock in the eastern Central Depression, is over 2000 m (Fig. 10). In summary, data in the

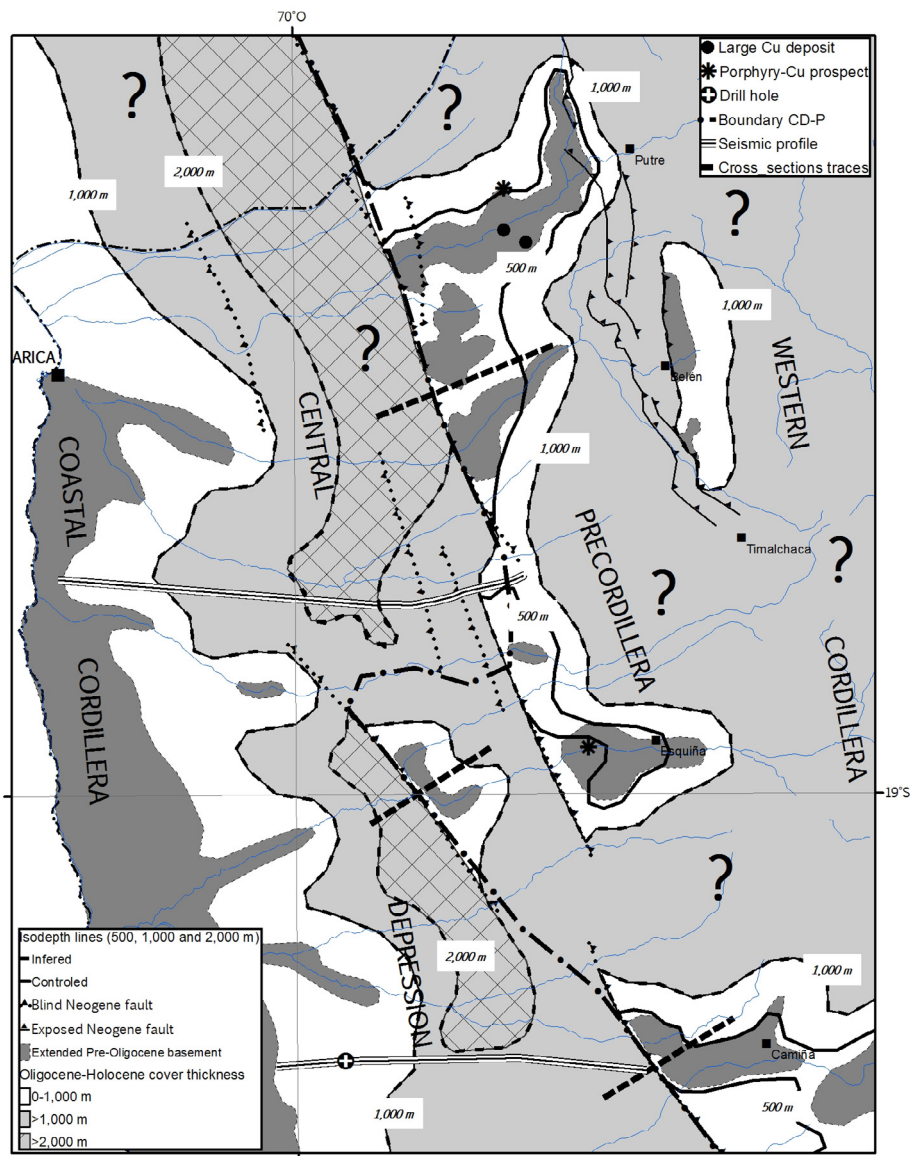


Fig. 10. Thickness distribution map of the Oligocene to Holocene post-mineral cover in the study area. The inferred area with more than 1000 m thickness is indicated with color. Note that in the Central Depression, two reflection seismic profiles exist and the 1000 and 2000 m isolines can be indicated, whereas to the east, the 500 m isoline can be determined, especially around the Precordillera canyons, the 1000 m isoline is inferred and the higher isolines are not known in the Western Cordillera. A semi-continuous strip with uplifted bedrock blocks and cover thickness thinner than 1000 m is accessible to deep exploration along the Paleocene to early Eocene porphyry-copper belt. Outcrops of the pre-Oligocene bedrock were gently exaggerated for better visualization purposes.

Central Depression allows approximation of the 1000 and 2000 m thickness isolines.

In the Precordillera, the cover thickness is observed along deeply incised valleys where the 500 and 1000 m thickness isolines can be drawn (Fig. 10). The data do not permit to infer the 2000 m and higher isolines. In the western border of the Precordillera, regional blind high-angle Oligocene to Miocene reverse faults have caused uplift, preservation and partial exposure of the bedrock hosting the Paleocene to early Eocene porphyry-Cu-Mo belt (Figs. 3, 6, 9 and 10). The bedrock is more elevated in the fault hanging walls (Precordillera) compared to the footwalls (eastern Central Depression) and its Oligocene offset is at least 300–900 m (Fig. 9). We assume that the longitudinal segments of faults that were activated during the Oligocene and Miocene were also the segments activated during the Eocene. In the western part of the Ausipar Fault hanging wall, the thickness of cover ranges from approximately 400 to 600 m, whereas in its eastern part, in the Lluta and Cardones valley, the thickness is small, varying from 0 to 500 m, and in the Azapa valley, the maximum thickness is observed (900 m). To the south, east of Codpa village, the Late Cretaceous to Paleocene intrusive bedrock is exposed in a valley bottom, at 150 m below the cover surface (Fig. 10). In the Camarones valley, the post-mineral cover thickness is less than 500 m, to the west of Esquiña village, and this increases to the west and to the east; in the Camarones prospect area, the thickness of cover is approximately 600 to 700 m. For the hanging wall of the Taltape Fault, the thickness of cover ranges from 600 to 900 m (Figs. 5, 9 and 10). To the south, in the Moquella Flexure area, the thickness of cover varies from 300 to 700 m (Figs. 9 and 10). To the east and south of the Camiña village, thickness remains at less than 500 m.

In the Western Cordillera, above the middle Eocene to early Oligocene metallogenic belt, there are few data for the post-mineral cover thickness. The thickness of the Oligo-Miocene formations is ca. 2500 m and each Miocene-Holocene strato-volcano can contribute up to 2000 m of thickness to the cover, therefore a maximum value of 4500 m can be locally reached. In addition, the Neogene structural shortening has produced substantial increases of the cover thickness. Nonetheless, the Oligocene-Holocene cover is deposited atop the eastern outcrops of the Belén Metamorphic Complex, and has not been faulted or folded extensively. Here, a restricted area has a cover less than 1000 m in thickness (Fig. 10). In general, the data permit to infer the 1000 m isoline whereas the higher isolines cannot be established.

Consequently, the cover thickness in the study area varies highly from 0 to more than 5000 m and increases globally from west to east. The cover thickness distribution map has different resolution depending of available information. Data allows approximation of the 1000 and 2000 m thickness isolines in the Central Depression and the 500 and 1000 m thickness isolines in the Precordillera (Fig. 10). In the Western Cordillera, cover thickness data are very limited and the 1000 m isoline is inferred and the higher isolines are not known. For the Paleocene to early Eocene metallogenic belt in the Precordillera, we distinguish a semi-continuous strip of uplifted bedrock blocks where the cover thickness is less than 500 to 1000 m (Fig. 10). The results imply that there is a large region accessible to exploration at <1000 m, but included are areas where larger thicknesses of cover may exist in deep paleovalleys. The cover thickness is strongly controlled by the sedimentation and volcanic production rates and by the effects of Eocene to Miocene contractional tectonic evolution.

6. Distribution of the magmatic and metallogenic belts

Based on the available geological information summarized herein we have constructed maps showing an improved distribu-

tion of the prospective magmatic and metallogenic belts and the places these belts may be amenable to exploration under shallow post-mineral cover. The Paleocene to early Eocene metallogenic belt is ca. 30 km wide and defined in the Precordillera by a discontinuous NNW-SSE strip of intrusions and related ore deposits or prospects that include veins, breccia-pipes and stockworks with copper, copper-molybdenum, copper-gold-silver and silver-lead-zinc metal assemblages. Two porphyry-Cu prospects (La Mancha and Camarones) have potassic and sericite alteration and mineralization associated with quartz-sulfide stockwork veinlets. The age for intrusion related to the major breccia deposit is 55.5 Ma and hydrothermal alteration ages in the larger deposits and one porphyry-Cu prospect are 69.5, 56.1 and 54.5 Ma. Additionally, large porphyry-Cu-Mo contemporaneous deposits immediately outside the area and the two porphyry-Cu prospects in the area, suggest a significant potential for ores beneath the post-mineral cover (Figs. 2, 8, and 10). To the west of the Paleocene to early Eocene metallogenic belt from Arica to Camiña (i.e. from 18.5 to 19.5°S), middle Cretaceous (99–85 Ma) intrusions associated with copper veins are locally exposed in a NW-oriented discontinuous strip. The southern projection of this middle Cretaceous belt south of 19°S overlaps with the Paleocene to early Eocene metallogenic belt (Fig. 8).

The middle Eocene to early Oligocene metallogenic belt is mainly defined by 46.3 to 44.4 Ma intrusions that are discontinuously distributed in the Western Cordillera, at the north and south extremes of the study area (Fig. 7). Only one small middle Eocene to early Oligocene Ag-(Pb, Zn, Cu) vein is present, but to the north and south of this, the contemporaneous porphyry-Cu belt is well developed (Fig. 2; Camus, 2003; Perelló et al., 2003; Sillitoe and Perelló, 2005). In the study area, the post-mineral cover is extremely extensive and thick (Fig. 10). An exception is the area of thin cover in the Belén-Tignámar area, in approximately 40 km long by 10 km wide. In this area, the Belén Metamorphic Complex is locally exposed, and thus there is potential for middle Eocene to early Oligocene ore deposits (Figs. 8 and 10). The width of this belt in northernmost Chile is unknown but according to projections from north and south, it can be estimated at approximately 40 km.

The youngest Miocene to early Pliocene metallogenic belt, in the study area, is well-exposed and formed by mainly small Au-Ag and polymetallic deposits, which are related to volcanic centers and diorite, quartz monzonite and dacite hypabyssal intrusions. The intrusion ages vary from 16.0 to 6.6 Ma and the alteration ages in deposits and prospects range from 18.9 to 9.3 Ma. The magmatic belt is evidently defined by stratovolcanoes with different degrees of preservation. The Miocene to early Pliocene magmatic and metallogenic belt at this latitude is very wide, ca. 50 km in the Western Cordillera of northern Chile and ca. 150 km in the Altiplano of western Bolivia.

At scale of the Andes, the different magmatic and metallogenic belts can be seen as parallel and continuous strips in that the younger are located progressively to east (Fig. 2; Sillitoe, 1988, 1992; Camus, 2003; Perelló et al., 2003; Sillitoe and Perelló, 2005). However, in southern Peru the Mesozoic to Cenozoic magmatic belts are non-parallel and are locally superimposed on one another (Mamani et al., 2010) and in the 250 km Andean arc segment we have investigated, the Cenozoic magmatic and metallogenic belts also overlaps. For example, the Miocene to early Pliocene metallogenic belt is clearly superimposed in a 40–50 km-wide-zone on the middle Eocene to early Oligocene metallogenic belt and locally on the Paleocene to early Eocene belt (Fig. 8). The positions of these magmatic and metallogenic belts in the Andes are thought to form as a result of arc migration as consequence of subduction processes, such as forearc subduction erosion and/or variation of the subduction angle (Mpodozis and Ramos, 1989; Sandeman et al., 1995; Kay et al., 1999, 2005; Kay

and Coira, 2009). The Paleocene to early Eocene belt is well-defined whereas the middle Eocene to early Oligocene belt is poorly exposed but can be drawn by projections from north and south. Thus a magmatic arc migration eastward has occurred during the early-middle Eocene (from 51 to 46 Ma). In northern Chile, this arc jump was of around 30 km and may have been associated with moderate erosion subduction of the fore-arc (Mpodozis and Ramos, 1989) but in southern Peru, the migration was of more than 120 km, accompanied of magmatism decreasing and was likely associated to subduction flattening which existed until the early Oligocene at *ca.* 32 Ma (Sandeman et al., 1995; Perelló et al., 2003; Mamani et al., 2010). In northernmost Chile, a magmatic calm is apparently present between *ca.* 39 and 25 Ma (García et al., 2004; Acosta et al., 2011; Valenzuela et al., 2014) although detrital U-Pb zircon ages in east-proceeding rocks of the Oligocene Azapa Formation suggest this magmatic gap began after, around 30–35 Ma (Wotzlaw et al., 2011) and is interpreted to represent a period of flat-slab subduction. Therefore, the subduction flattening was initiated in southern Peru at *ca.* 51–46 Ma and was migrating southward, to presently central Chile, and would be associated to subduction of the NE-trending oceanic Juan Fernandez Ridge (James and Sack, 1999; Martinod et al., 2010). The late Eocene to early Oligocene porphyry-Cu-Mo deposits were emplaced along compressional and transpressional fault systems, that accompanied the formation of the Bolivian orocline, crustal thickening, strong inter-plate mechanical coupling, increased forearc subduction erosion and slab shallowing (Mpodozis and Cornejo, 2012). The overlap of the Miocene to early Pliocene metallogenic belt atop the earlier belts may be explained by renewed magmatism and maximum migration westward of the volcanic front, since *ca.* 32 Ma in southern Peru and since *ca.* 25 Ma in northernmost Chile, as consequence of subduction slab steepening (Sandeman et al., 1995; James and Sack, 1999; Kay et al., 1999; Kay and Coira, 2009). Additional geochronology studies of igneous rocks in the 17.5–19.5°S and around would help improve the understanding of the positions of the magmatic and metallogenic belts and their durations, and aid in prospecting.

7. Conclusions and implications

The northernmost Chilean Andes (17.5–19.5°S) include the projections of both the Paleocene to early Eocene and middle Eocene to early Oligocene arc-parallel metallogenic belts that contain giant porphyry-Cu-Mo deposits to the south in northern Chile and to the north in southern Peru. The Paleocene to early Eocene belt at 17.5–19.5°S is estimated to be 30-km wide in the Precordillera, where is well-defined by several intrusions, Cu veins and breccias and porphyry Cu-Mo prospects. The age for intrusion related to the major breccia deposit is 55.5 Ma and hydrothermal alteration ages in the major Cu vein deposit and one porphyry-Cu prospect range from 69.5 to 54.5 Ma. This belt is flanked to the east by the middle Eocene to early Oligocene belt that is associated with intrusions of 46.3–44.4 Ma and estimated to be 40-km wide in the Western Cordillera. The Miocene to early Pliocene metallogenic belt is the youngest arc-parallel zone of polymetallic mineralization and also dominantly occurs in the Western Cordillera where is well-exposed and wide (>50 km) extending east into the Bolivia. Available hydrothermal alteration ages in this belt vary from 18.9 to 9.3 Ma and intrusion ages, from 16 to 6.6 Ma. The Paleocene to early Oligocene belts are highly prospective for porphyry Cu-Mo deposits, but are largely covered by post-mineral sedimentary and volcanic rocks.

The Oligocene-Holocene cover is formed of continental sedimentary and pyroclastic volcanic successions in the west, and volcanic effusive and pyroclastic deposits and locally sedimentary

successions with local Miocene intrusions in the east. The thickness of this cover is highly variable, from 0 to 5000 m and decreases globally from east to west reflecting source volcanoes and eroding high elevation sources of sedimentary materials in the Cordillera to the east. The cover thickness distribution is strongly controlled by volcanism and sediment sources but also by the Eocene and younger contractional tectonic evolution, especially in the Precordillera. The cover sequence originally dipped gently to the west, but has been subsequently deformed by reverse and local thrust faults and wide amplitude anticlines and monoclines that are oriented north-northwest by south-southeast and are 30 to 60 km long. The dominant structures are steeply east-dipping (on average 60°) reverse faults which are mainly blind and have recurrent activity since the Eocene. The bedrock vertical displacement, during the Oligocene, is at least 300 to 900 m. The faults may include original offset in the middle Cretaceous period, but most of the movement may have constrained to be Incaic (late Eocene to early Oligocene) as documented in the Domeyko fault zone to the south and in southern Peru (Maksaev, 1979; Noble et al., 1979; Mégard, 1984, 1987; Reutter et al., 1991, 1996; Noblet et al., 1996; Maksaev and Zentilli, 1999; Tomlinson et al., 2001, 2015; Charrier et al., 2007, 2013; Mpodozis and Cornejo, 2012). In the study area, these faults have significant uplift in their hanging walls that both locally exposed basement rocks and also led to erosion or non-deposition of the Oligocene-Holocene cover sequence.

Our estimates of the current cover thicknesses were based on the exposures of basement-cover contact, the stratigraphic thicknesses and attitudes of the cover sequence, and cross-sections and geophysical data (Fig. 10). A significant result of these reconstructions is that much of the Paleocene to early Eocene metallogenic belt in the Precordillera is covered by less than 1000 m of cover and is therefore amenable to exploration for porphyry Cu-Mo deposits. In contrast, most of the middle Eocene to early Oligocene metallogenic belt lying to the east is concealed by more than 2000 m of cover with the exception of the areas surrounding the uplifted and exposed Belén Metamorphic Complex. The map of cover thickness superimposed on the position of the three metallogenic belts at 17.5–19.5°S represents a first attempt to assess prospectivity using the assumption that surface geology and subsurface geophysics and testing by drilling are relatively effective and economic to depths of 1000 m. In the future, improved estimates of the cover thickness can be accomplished by drilling and geophysical studies, and by improved geological mapping and projections of paleo-canyons filled with cover rocks.

In the Andean segment studied here and in southern Peru, the positions of magmatic and metallogenic belts remain poorly defined because of the extensive cover. Nonetheless, the belts do not form simple parallel arrays, and are locally superimposed on one another. For example, in northernmost Chile our data show that the Miocene to early Pliocene belt is superimposed on 40–50 km width of the Paleocene to early Oligocene belts. This overlap may be explained by renewed magmatism and maximum migration westward of the volcanic front, since *ca.* 25 Ma, as consequence of subduction slab steepening, following a period of magmatic calm and flat subduction from *ca.* 30–35 to 25 Ma.

Acknowledgments

Fieldwork and laboratory data considered in this study were mostly funded by the Chilean “Servicio Nacional de Geología y Minería” (SERNAGEOMIN) and the French “Institut de Recherche pour le Développement” (IRD). Interpretation and discussion of the data, as well as preparation of the manuscript, were made possible by the support of the Advanced Mining Technology Center (AMTC) of the “Universidad de Chile”, funded by the FB0809

program of CONICYT. We acknowledge specially to colleagues, D. Pacci and H. Munster, who read the manuscript and collaborated with unpublished information of certain prospects improving the work. The available reflection seismic profiles were generously facilitated by "Empresa Nacional del Petróleo" (ENAP) and were interpreted by M.G., Y. Simicic and N. Labbé. Likewise, we acknowledge the discussions with C. Mpodozis, A. Tomlinson, D. Sellés and R. Charrier, as well as the editorial revision of R. Tosdal and F. Pirajno.

References

- Acosta, H., Alván, A., Mamani, M., Oviedo, M., Rodríguez, J., 2011. Geología de los cuadrángulos de Pachía (36-v) y Palca (36-x), escala 1:50 000. INGEMMET, Boletín, Serie A: Carta Geológica Nacional 139: 100 p., 7 mapas.
- Aguirre, E., 1990. Geología del Complejo Volcánico Choquemilpe-Ajoya, Altiplano de Arica, I Región. Memoria de Título. Depto. de Geología, U. de Chile, 150p.
- Allmendinger, R.W., González, G., 2010. Invited review paper: neogene Quaternary tectonics of the coastal Cordillera, northern Chile. *Tectonophysics* 495, 93–110.
- Alpers, C., Brimhall, G., 1988. Middle Miocene climatic change in the Atacama Desert, northern Chile: Evidence from supergene mineralization at La Escondida. *G.S.A. Bull.* 100, 1640–1656.
- Arancibia, G., Matthews, S.J., Pérez de Arce, C., 2006. K-Ar and 40Ar/39Ar geochronology of supergene processes in the Atacama Desert, Northern Chile: tectonic and climatic relations. *J. Geol. Soc.* 163, 107–118.
- Argandoña, R., 1984. Geología del cuadrángulo Cerro Socora y características generales del área geotermal de Puchuldiza. Memoria de Título (inédito), Departamento de Geología, Universidad de Chile, Santiago.
- Basel, M.A., Charrier, R., Hervé, F., 1996. New Ages (U-Pb, Rb-Sr, K-Ar) From Supposed Pre-Cambrian Units in Northern Chile: Some Geotectonic Implications. Third ISAG, Saint Malo, France.
- Bennett, M., Gollan, M., Staubmann, M., Bartlett, J., 2014. Motive, means, and opportunity: key factors in the discovery of the nova-bollinger magmatic nickel-copper sulfide deposits in Western Australia. *Soc. Econ. Geol. Special Publication* 18, 301–320.
- Bisso, C., 1991. Geología Y Geoquímica Del Yacimiento De Oro Y Plata Choquemilpe. Memoria de Título. Depto. de Geología, U. de Chile, I Región, Chile, p. 134.
- Bouzari, F., Clark, A., 2002. Anatomy, evolution, and metallogenetic significance of the supergene orebody of the Cerro Colorado porphyry copper deposit, I Región, Northern Chile. *Econ. Geol.* 97, 1701–1740.
- Brimhall, G.H., Dilles, J.H., Proffett, J.M., 2006. The role of geologic mapping in mineral exploration: society of Economic Geologists Special Publication 12, 221–241.
- Calvo, M., 1992. Informe geológico de visita realizada a Mina Guanaco, sector de Belén. Informe inédito, 5 p.
- Camus, F., 2003. Geología De Los Sistemas Porfíricos En Los Andes De Chile. Servicio Nacional de Geología y Minería, Santiago.
- Cecioni, G., García, F., 1960. Stratigraphy of coastal range in Tarapacá Province, Chile. *Bull. Am. Assoc. Pet. Geol.* 44 (10), 1609–1620.
- Cecioni, A., Cornejo, P., Ruz, L., 2000. Choquemilpe, un yacimiento epitermal de oro y plata, relacionado al núcleo de un estratovolcán. Actas IX Congreso Geológico Chileno, vol. 1, p. 181–183. Puerto Varas, Chile.
- Charrier, R., Pinto, L., Rodríguez, M.P., 2007. Tectonostratigraphic evolution of the Andean Orogen in Chile. In: Moreno, T., Gibbons, W., (Eds.), *The Geology of Chile*. Geological Society of London, pp. 21–114.
- Charrier, R., Héral, G., Pinto, L., García, M., Riquelme, R., Farias, M., Muñoz, N., 2013. Cenozoic tectonic evolution in the Central Andes in northern Chile and west-central Bolivia. Implications for paleogeographic, magmatic and mountain building evolution. *Int. J. Earth Sci. (Geol. Rundsch.)* 102, 235–264. <http://dx.doi.org/10.1007/s00531-012-0801-4>.
- Clark, A., Farrar, E., Kontak, D., Langridge, R., Arenas, M., France, L., McBride, S., Woodman, P., Wasteneys, H., Sandeman, H., Archibald, D., 1990. Geologic and geochronologic constraints on the metallogenetic evolution of the Andes of southeastern Peru. *Econ. Geol.* 85, 1520–1583.
- Cortés, J., Castruccio, A., Cascante, M.; 2014. Geología del área del Volcán Isluga. Región de Tarapacá. Servicio Nacional de Geología y Minería, Carta Geológica de Chile, Serie Geología Básica, 1 map at scale 1:100.000, Santiago, Chile.
- Cruzat, A., 1967. Yacimientos de manganeso del Departamento de Arica, Tarapacá, Chile. Instituto de Investigaciones Geológicas – Junta de Adelanto de Arica. Unpublished report. 7 vols. Arica, Chile.
- Cruzat, 1970. Genesis of manganese deposits in Northern Chile. *Econ. Geol.* 65, 681–689.
- Evenstar, L., Hartley, A., Stuart, F., Mather, A., Rice, C., Chong, G., 2009. Multiphase development of the Atacama Planation Surface recorded by cosmogenic ^{3}He exposure ages: Implications for uplift and Cenozoic climate change in western South America. *Geology* 37 (1), 27–30.
- Farias, M., Charrier, R., Comte, D., Martinod, J., Héral, G., 2005. Late Cenozoic uplift of western flank of the Altiplano: evidence from the depositional, tectonic and geomorphologic evolution and shallow seismic activity (northern Chile at 19°30' S°). *Tectonics*, 24, TC4001, doi:<http://dx.doi.org/10.1029/2004TC001667>.
- Galli, C., Dingman, R., 1962. Cuadrángulos Pica, Alca, Matilla y Chacarilla, con un estudio de aguas subterráneas. Instituto de Investigaciones Geológicas, Carta Geológica de Chile, Provincia de Tarapacá, 7-10: 123 p.
- García, F., 1967. Geología del Norte Grande de Chile. In *Symposium sobre el Geosinclinal Andino*. Sociedad Geológica de Chile, No. 3: 138 p. Santiago (1962).
- García, M., 1996. Geología Y Estructura Del Borde Del Altiplano Occidental, En El Área De Belén (Chile). Depto. de Geología, U. de Chile, Tesis de Magíster y Memoria de Título, p. 111.
- García, M., 2002. Evolution oligo-néogène de l'Altiplano occidental (arc et avant-arc du Nord du Chili, Arica). Tectonique, volcanisme, sédimentation, géomorphologie et bilan érosion-sédimentation. *Géologie Alpine, Mémoire H.* S. N° 40 (Thèse de doctorat), Université Joseph Fourier (Grenoble, France). 118 p.
- García, M., Fuentes, G., 2012. Carta Cuya, Regiones de Arica y Parinacota y de Tarapacá. Servicio Nacional de Geología y Minería, Carta Geológica de Chile, Serie Geología Básica, N° 146, 80 p., 1 mapa escala 1:100.000. Santiago, Chile.
- García, M., Héral, G., 2005. Fault-related folding, drainage network evolution and valley incision during the Neogene in the Andean Precordillera of Northern Chile. *Geomorphology* 65, 279–300.
- García, M., Gardeweg, M., Héral, G., Pérez de Arce, C., 2000. La Ignimbrita Oxaya y la Caldera Lauca: un evento explosivo de gran volumen del Mioceno Inferior en la región de Arica (Andes Centrales; 18–19° S). *Actas IX Congreso Geológico Chileno, Puerto Varas 2*, 286–290.
- García, M., Gardeweg, M., Clavero, J., Héral, G., 2004. Hoja Arica, Región de Tarapacá. Servicio Nacional de Geología y Minería, Carta Geológica de Chile, Serie Geología Básica, N° 84, 150 p., 1 mapa escala 1:250.000. Santiago, Chile.
- García, M., Riquelme, R., Farias, M., Héral, G., Charrier, R., 2011. Late Miocene-Holocene canyon incision in the western Altiplano, northern Chile: tectonic or climatic forcing? *J. Geol. Soc. (London)* 168, 1047–1060.
- García, M., Clavero, J., Gardeweg, M., 2012. Cartas Visviri y Villa Industrial, Región de Arica y Parinacota. Servicio Nacional de Geología y Minería, Carta Geológica de Chile, Serie Geología Básica, N°s 135–136, 43 p., 1 mapa escala 1:100.000. Santiago, Chile.
- García, M., Fuentes, G., Riquelme, F., 2013. Carta Miñimiñi, Regiones de Arica y Parinacota y de Tarapacá. Servicio Nacional de Geología y Minería, Carta Geológica de Chile, Serie Geología Básica, N° 157, 1 mapa escala 1:100.000. Santiago, Chile.
- Gardeweg, M., 1996. Estudio geológico-volcanológico preliminar de los prospectos Vilañumani y Padre Jiguata, Altiplano de Arica. Internal report, BHP Billiton Chile S.A., 51 p., 4 appendices.
- Gröpper, H., Calvo, M., Crespo, H., Bisso, C., Cuadra, W., Dunkerley, P., Aguirre, E., 1991. The epithermal gold-silver deposit of Choquemilpe, Northern Chile. *Econ. Geol.* 86, 1206–1221.
- Harambourg, S., 1990. Geología Pre-Cenozoica De La Cordillera De Los Andes Entre Las Quebradas Aroma Y Juan De Morales. Memoria de Título, Departamento de Geología, Universidad de Chile, I Región, p. 228.
- James, D.E., Sacks, I.S., 1999. Cenozoic formation of the Central Andes: A geophysical perspective. In: Skinner, B.J. (Ed.), *Geology and Ore Deposits of the Central Andes*. Society of Economic Geologists Special Publication, pp. 1–25.
- Jordan, T., Kirk-Lawlor, N., Blanco, N., Rech, J., Cosentino, N., 2014. Landscape modification in response to repeated onset of hyperarid paleoclimate states since 14 Ma, Atacama Desert, Chile. *GSA Bull.* 126, 1016–1046.
- Kay, S.M., Coira, B., 2009. Shallowing and steepening subduction zones, continental lithosphere loss, magmatism and crustal flow under the central Andean Altiplano-Puna plateau. *Geol. Soc. Am. Mem.* 204, 229–260.
- Kay, S.M., Godoy, E., Kurtz, A., 2005. Episodic arc migration, crustal thickening, subduction erosion, and magmatism in the south-central Andes. *Geol. Soc. Am. Bull.* 117, 67–88. <http://dx.doi.org/10.1130/B25431.1>.
- Kay, S.M., Mpodozis, C., Coira, B., 1999. Magmatism, tectonism and mineral deposits of the Central Andes (22°–33°S latitude). *Soc. Econ. Geol. Special Publication* 7, 27–59.
- Kirk-Lawlor, N., Jordan, T., Rech, J., Lehmann, S., 2013. Late Miocene to Early Pliocene paleohydrology and landscape evolution of Northern Chile, 19° to 20° S. *Palaeogeogr. Palaeoclimatol. Palaeoecol.* 387, 76–90.
- Kött, A., Gaupp, R., Wörner, G., 1995. Miocene to Recent history of the Western Altiplano in Northern Chile revealed by lacustrine sediments of the Lauca Basin (18°15'–18°40'S/69°30'–69°05' W). *Geol. Rundsch.* 84, 770–780.
- Lahsen, A., 1982. Upper Cenozoic volcanism and tectonism in the Andes of northern Chile. *Earth Sci. Rev.* 18, 285–302.
- Loewy, S., Connelly, J., Dalziel, I., 2004. An orphaned Basement block: The Arequipa-Antofalla basement of the central Andean margin of South America. *GSA Bull.* 116, 171–187.
- Lucassen, F., Beccio, R., Wilke, H.G., Franz, G., Thirlwall, M.F., Viramonte, J., Wemmer, K., 2000. Proterozoic-Paleozoic development of the basement of the Central Andes (18–26°S) – a mobile belt of the South American craton. *J. S. Am. Earth Sci.* 13 (8), 697–715.
- Maksaev, V., 1978. Cuadrángulo Chitigua y sector oriental del Cuadrángulo Cerro Palpana, Región de Antofagasta. Instituto de Investigaciones Geológicas, Carta Geológica de Chile, 31, escala 1:50.000, 55 p.
- Maksaev, V., 1979. Las fases tectónicas Incaica y Quechua en la Cordillera de los Andes del Norte Grande de Chile. II Congreso Geológico de Chile, B64–B77.
- Maksaev, V., Zentilli, M., 1999. Fission track thermochronology of the Domeyko Cordillera, northern Chile: implications for Andean tectonics and porphyry copper metallogenesis. *Explor. Mining Geol.* 8, 65–89.
- Maksaev, V., Townley, B., Palacios, C., Camus, F., 2007. Metallic ore deposits. In: Gibbons, W., Moreno, T. (Eds.), *The Geology of Chile*. The Geological Society, London, pp. 179–199.

- Mamani, M., Wörner, G., Sempere, T., 2010. Geochemical variations in igneous rocks of the Central Andean orocline (13° S to 18° S): Tracing crustal thickening and magma generation through time and space. *Geol. Soc. Am. Bull.* 122, 162–182.
- Manske, S.L., Paul, A.H., 2002. Geology of a major new porphyry copper center in the Superior (Pioneer) district, Arizona. *Econ. Geol.* 97, 197–220.
- Martinod, J., Husson, L., Roperch, P., Guillaume, B., Espurt, N., 2010. Horizontal subduction zones, convergence velocity and the building of the Andes. *Earth Planet. Sci. Lett.* 299, 299–309.
- McCuig, T.C., Hronsky, J., 2014. The mineral system concept: the key to exploration targeting. *Soc. Econ. Geol. Special Publication* 18, 153–175.
- Mégard, F., 1984. The Andean orogenic period and its major structures in Central and Northern Peru. *J. Geol. Soc. London* 141, 893–900.
- Mégard, F., 1987. Cordilleran Andes and marginal Andes: a review of Andean geology north of the Arica Elbow (18° S). In: Monger, J.W.H., Francheteau, J., (Eds.), Circum-Pacific orogenic belts and evolution of the Pacific ocean basin. *Am. Geophys. Union, Geodynamics Series*, 18, pp. 71–95.
- Morandé, J., Gallardo, F., Muñoz, M., Farias, M., 2015. Carta Guaviña. Región de Tarapacá. Servicio Nacional de Geología y Minería, Carta Geológica de Chile, Serie Geología Básica, No. 177, 1 mapa escala 1:100.000. Santiago.
- Mordovich, C., 1965. Reseña sobre las exploraciones petrolíferas de la ENAP en la zona norte, años 1956 a 1962. *Minerales* 20 (89), 32–61.
- Mortimer, C., 1980. Drainage evolution in the Atacama Desert of Northern Chile. *Revista Geológica de Chile* (11), 3–28.
- Mortimer, C., Saric, N., 1972. Landform evolution in the coastal region of Tarapacá Province. *Chile. Rev. Géomorphol. Dynamique* 21, 162–170.
- Mortimer, C., Farrar, E., Saric, N., 1974. K-Ar ages from Tertiary lavas of the northernmost Chilean Andes. *Geol. Rundschau* 63, 484–489.
- Mpodozis, C., Cornejo, P., 2012. Cenozoic tectonics and porphyry copper systems of the Chilean Andes. *Soc. Econ. Geol. Special Publication* 16, 329–360.
- Mpodozis, C., Ramos, V., 1989. The Andes of Chile and Argentina. Houston, Texas, Circum-Pacific council for Energy and Minerals Resources. *Earth Sci. Ser.* 11, 59–90.
- Münchmeyer, C., 1996. Exotic deposits—products of lateral migration of supergene solutions from porphyry copper deposits. *Soc. Econ. Geol. Special Publication* 5, 43–58.
- Muñoz, N., Charrier, R., 1996. Uplift of the western border of the Altiplano on a west-vergent thrust system, Northern Chile. *J. South Am. Earth Sci.* 9, 171–181.
- Muñoz, N., Elgueta, S., Harambour, S., 1988. El Sistema Jurásico (Formación Livilcar) en el curso superior de la quebrada Azapa, I Región: Implicancias paleogeográficas. *Actas V Congreso Geológico Chileno*, Santiago, Tomo 1, pp. A403–A415.
- Muzzio, G., 1986. Geología de los cuadrángulos Caleta Camarones, Cuya, Punta Gorda y Atajaña. Servicio Nacional de Geología y Minería. Informe inédito, 43 p., 1 mapa escala 1:100.000.
- Naranjo, J.A., Paskoff, R., 1985. Evolución cenozoica del piedemonte andino en la Pampa del Tamarugal, Norte de Chile (18° – 21° S). In: *Actas IV Congreso Geológico Chileno, Antofagasta*, pp. 149–164. V. 5.
- New, M., Lister, D., Hulme, M., Makin, I., 2002. A high-resolution data set of surface climate over global land areas. *Clim. Res.* 21, 1–25.
- Noble, D.C., McKee, E.H., Mégard, F., 1979. Early Tertiary "Incaic" tectonism, uplift and volcanic activity, Andes of central Peru. *Geol. Soc. Am. Bull.* 90, 903–937.
- Noblet, C., Lavenu, A., Marocco, R., 1996. Concept of continuum as opposed to periodic tectonism in the Andes. *Tectonophysics* 255, 65–78.
- Ordóñez, A., Rivera, C., 2004. Mapa Metalógénico de la I Región de Tarapacá. Escala 1:500.000. Geodatos y Servicio Nacional de Geología y Minería, Santiago. 37 p. volúmenes.
- Pacci, D., 1970. *Prospección Geológica Y Estudio Geoquímico En La Zona De Alteración De Tignamar. Memoria de Título, Departamento de Geología, Universidad de Chile, Departamento de Arica*, p. 66.
- Pacci, D., 1977. Estudios realizados en la zona de alteración hidrotermal de Tignamar, Provincia de Arica. Instituto de Investigaciones Geológicas. Informe inédito, 19 p., Arica, Chile.
- Pacci, D., 1978. *Reconocimiento geológico del Proyecto Camarones, Provincia de Arica. Instituto de Investigaciones Geológicas, Informe inédito (1226)*. 23 p. Santiago.
- Pacci, D., Hervé, F., Munizaga, F., Kawashita, K., Cordani, U., 1980a. Acerca de la edad Rb/Sr precámbrica de rocas de la Formación Esquistos de Belén, Departamento de Parinacota, Chile. *Revista Geológica de Chile*, N° 11, p. 43–50.
- Pacci, D., Cáceres, R., Sayes, J., 1980b. Inventario de yacimientos metálicos y no-metálicos. Primera Región de Tarapacá. Instituto de Investigaciones Geológicas. Informe inédito (2029). 5 vols., 903 p. Santiago.
- Pacci, D., Hervé, F., Munizaga, F., Kawashita, K., 1981. Edades radioisotópicas paleógenas del Granito de Tawaicoñu, Altiplano de Arica, 31. Universidad de Chile, Comunicaciones.
- Perelló, J., Carlotto, V., Zárate, A., Ramos, P., Posso, H., Neyra, C., Caballero, A., Fuster, N., Muhr, R., 2003. Porphyry-style alteration and mineralization of the middle Eocene to early Oligocene Andahuaylas-Yauri belt, Cuzco region, Peru. *Econ. Geol.* 98, 1575–1605.
- Pinto, L., Hérial, G., Charrier, R., 2004. Sedimentación sintectónica asociada a las estructuras neógenas en la Precordillera de la zona de Moquegua, Tarapacá ($19^{\circ}15'$ S, norte de Chile). *Revista Geológica de Chile* 31 (1), 19–44.
- Quang, C.X., Clark, A.H., Lee, J.K.W., Hawkes, N., 2005. Response of supergene process to episodic Cenozoic uplift, pediment erosion, and ignimbrite eruption in the porphyry copper province of Southern Peru. *Econ. Geol.* 100, 87–114.
- Rech, J.A., Currie, B.S., Michalski, G., Cowan, A.M., 2006. Neogene climate change and uplift in the Atacama Desert, Chile. *Geology* 34 (9), 761–764.
- Reutter, K.J., Scheuber, E., Helmke, D., 1991. Structural evidence of orogen-parallel strike-slip displacements in the Precordillera of northern Chile. *Geol. Rundsch.* 80 (1), 135–153.
- Reutter, K., Scheuber, E., Chong, G., 1996. The Precordillera fault system of Chuquicamata, Northern Chile: evidence for reversals along arc-parallel strike-slip faults. *Tectonophysics* 259, 213–228.
- Riquelme, R., 1998. *Evolución Tectonosedimentaria Post-Oligocénica Del Bordo Occidental Del Altiplano, Entre Tignamar Y El Salar De Surire, I Región, Chile. Tesis de Magíster y Memoria de Título, Departamento de Geología, U. de Chile*, p. 123.
- Riquelme, F., 2015. Modelamiento de la deformación mezo-cenozoica en el borde occidental del Altiplano chileno, área de Suca-Camiña (19.3° S). *Memoria de Título, Departamento de Geología, U. de Chile*, 58 p.
- Salas, R., 1966a. Breve informe geológico de la Mina Santa Ana, quebrada de Camarones, Departamento de Arica. Instituto de Investigaciones Geológicas-Empresa Nacional de Minería. Informe inédito, 4 p.
- Salas, R., 1966b. Recomendaciones y sugerencias para catesos y prospecciones en la Mina Santo Domingo y vetas vecinas de la Compañía Minera San Carlos y Mina Taltape. Instituto de Investigaciones Geológicas-Compañía Minera San Carlos. Informe inédito, 6 p.
- Salas, R., Kast, R., Montecinos, F., Salas, I., 1966. *Geología y recursos minerales del Departamento de Arica, Provincia de Tarapacá*. Instituto de Investigaciones Geológicas. Boletín. 21, 130 p.
- Sánchez, M., 1970. *Geología Del Distrito Argentífero De Choquelimpie*. Instituto de Investigaciones Geológicas (Santiago), Informe inédito, p. 35.
- Sandeman, H.A., Clark, A.H., Farrar, E., 1995. An integrated tectonomagmatic model for the evolution of the southern Peruvian Andes (13 – 20° S) since 55 Ma. *Int. Geol. Rev.* 37, 1039–1073.
- Saric, N., Mortimer, C., 1971. Apuntes Sobre Las Minas Santa Ana, Lucita Y Taltape, Provincia De Tarapacá. Departamento de Arica. Instituto de Investigaciones Geológicas, Informe inédito, p. 7.
- Sayes, J., 1977. *Estudio Geológico De Yacimientos Metálicos Del Sector Belén-Tignamar*. Instituto de Investigaciones Geológicas (Arica), Informe inédito, p. 48.
- Sébrier, M., Lavenu, A., Fornari, M., Soulás, J., 1988. Tectonics and uplift in Central Andes (Perú, Bolivia and Northern Chile) from Eocene to present. *Géodynamique* 3 (1–2), 85–106.
- Sillitoe, R., 1988. Epochs of intrusion-related copper mineralization in the Andes. *J. South Am. Sci.* 1, 89–108.
- Sillitoe, R., 1992. Gold and copper metallogeny of the Central Andes, past, present, and future exploration objectives. *Econ. Geol.* 87, 2205–2216.
- Sillitoe, R., 2005. Supergene oxidized and enriched porphyry copper and related deposits. *Econ. Geol.* 100th Anniversary Volume, 723–768.
- Sillitoe, R.H., McKee, E.H., 1996. Age of supergene oxidation and enrichment in the Chilean porphyry copper province. *Econ. Geol.* 91, 164–179.
- Sillitoe, R.H., Mortensen, J.K., 2010. Longevity of porphyry copper formation at Quellaveco, Peru. *Econ. Geol.* 105, 1157–1162.
- Sillitoe, R.H., Perelló, J., 2005. Andean copper province: tectonomagmatic settings, deposit types, metallogeny, exploration, and discovery. *Econ. Geol.* 100, 845–890.
- Sillitoe, R.H., Thompson, J.F.H., 2006. Changes in mineral exploration practice: consequences for discovery. *Soc. Econ. Geol. Special Publication* 12, 193–219.
- Simmons, A., Tosdal, R.M., Wooden, J.L., Mattos, R., Concha, O., McCracken, S., Beale, T., 2013. Punctuated magmatism associated with Paleocene to Eocene porphyry Cu deposits of southern Peru. *Econ. Geol.* 108, 625–630.
- Strecker, M., Alonso, R.N., Bookhagen, B., Carrapa, B., Hilley, G.E., Sobel, E.R., Trauth, M.H., 2007. Tectonics and Climate of the Southern Central Andes. *Annu. Rev. Earth Planet. Sci.* 35, 747–787.
- Tobar, A., Salas, I., Kast, R., 1968. Cuadrángulos Camaraca y Azapa. Provincia de Tarapacá. Instituto de Investigaciones Geológicas, Carta Geol. de Chile, N°s 19 y 20, escala 1:50.000, 13 p.
- Tomlinson, A., Blanco, N., Maksaev, V., Dilles, J., Grunder, A., Ladino, M., 2001. *Geología de la Precordillera Andina de Quebrada Blanca-Chuquicamata, Regiones I y II (20°30'–22°30' S)*. Servicio Nacional de Geología y Minería (Chile). Informe registrado IR-01-20, 2 vols., 444p., 20 mapas escala 1:50.000.
- Tomlinson, A., Blanco, N., Ladino, M., 2015. Carta Mamiña, Región de Tarapacá. Servicio Nacional de Geología y Minería, Carta Geológica de Chile, Serie Geología Básica 174: 183 p., 1 mapa escala 1:100.000. Santiago.
- Valenzuela, I., Herrera, S., Pinto, L., del Real, I., 2014. Carta Camiña, Regiones de Arica y Parinacota y de Tarapacá. Servicio Nacional de Geología y Minería, Carta Geológica de Chile, Serie Geología Básica, No. 170, 1 mapa escala 1:100.000. Santiago.
- Wilson, J., García, W., 1962. Geología de los cuadrángulos de Pachía y Palca. Com. Carta Geol. Nac., Boletín N° 4, 82 p. Escala 1:100.000. Lima, Perú.
- Wörner, G., Harmon, R.S., Davidson, J., Moorbat, S., Turner, D.L., McMillan, N., Nye, C., Lopez-Escobar, L., Moreno, H., 1988. The Nevados de Payachata volcanic region (18° S/ 69° W, N. Chile). I. Geological, geochemical, and isotopic observations. *Bull. Volcanol.* 50 (5), 287–303.
- Wörner, G., Hammerschmidt, K., Henjes-Kunst, F., Lezaun, J., Wilke, H., 2000a. Geochronology (Ar-Ar, K-Ar and He-exposure ages) of Cenozoic magmatic rocks from northern Chile (18 – 22° S): Implications for magmatism and tectonic evolution of the central Andes. *Revista Geológica de Chile* 27, 205–240.
- Wörner, G., Lezaun, J., Beck, A., Heber, V., Lucassen, F., Zinggbe, E., Rössling, R., Wilke, H.G., 2000b. Precambrian and Early Paleozoic evolution of the Andean

- basement at Belén (northern Chile) and Cerro Uyarani (western Bolivia Altiplano). *J. S. Am. Earth Sci.* 13 (8), 717–737.
- Wotzlaw, J., Decou, A., von Eynatten, H., Wörner, G., Frei, D., 2011. Jurassic to Palaeogene tectono-magmatic evolution of northern Chile and adjacent Bolivia from detrital zircon U-Pb geochronology and heavy mineral provenance. *Terra Nova* 23, 399–406.
- Zappettini, E., Miranda-Angles, V., Rodríguez, C., Palacios, O., Cocking, R., Godeas, M., Uribe-Zeballos, H., Vivallo, W., Paz, M., Seggiaro, R., Heuschmidt, B., Gardeweg, M., Boulanger, E., Korzeniewski, L., Mpodozis, C., Carpio, M., Rubiolo, D. 2001. Mapa Metalógenico de la Región Fronteriza entre Argentina, Bolivia, Chile y Perú (14°S-28°S). Servicio Nacional de Geología y Minería, Publicación Geológica Multinacional, No 2, 222 p. 1 mapa escala 1:1.000.000. Santiago.